Submitted to Physica A

LBL-8300
Preprint

THE USE OF ANTICOMMUTING INTEGRALS IN STATISTICAL MECHANICS II

Stuart Samuel

October 1978

Prepared for the U. S. Department of Energy
under Contract W-7405-ENG-48

DISCLAIMER

THE USE OF ANTICOMMUTING INTEGRALS IN STATISTICAL MECHANICS II*

Stuart Samuel

Lawrence Berkeley Laboratory
University of California
Berkeley, California 94720

October 9, 1978

ABSTRACT

This paper deals with the following exactly solvable two dimensional statistical mechanics problems: The Ising model, the free fermion model, and close-packed dimer problems on various lattices. The emphasis is on graphical calculational techniques. Using them, the partition functions of the Ising and free fermion models are rederived. A diagrammatic set of rules is obtained which allows one to quickly calculate the partition functions of a wide class of dimer problems. Finally, I present a simple procedure to calculate the vacuum expectation value of an arbitrary product of Ising spin variables.

*Work has been supported by the High Energy Physics Division of the United States Department of Energy.

I. INTRODUCTION

In the first paper[1]) (to be referred to as I) certain partition functions are represented as fermionic-like lattice field theories using Grassmann integrals. This allows one to use powerful field theory methods to attack statistical mechanics problems. Several models had quadratic action representations. Among these were the two-dimensional Ising model and the two-dimensional square lattice dimer problem. They are pseudo-free theories and are exactly solvable. In this paper, these two partition functions are explicitly computed (Sec. II). This is a straightforward calculation: one transforms to momentum space just as one would do with a free field theory. This partically diagonalizes the problem; it breaks up into a product of 4 x 4 determinants. Next, graphical methods are introduced to organize the algebra (Sec. III). They are useful because they are systematic and pictorial. Section IV considers the general class of solvable 2-dimensional close-packed dimer problems on various lattices. A set of rules are derived which quickly compute partition functions. These rules are illustrated using the square lattice and applied to the hexangonal lattice. Next, the rules are extended to general pseudo-free theories. This means that, given any quadratic action, there is a simple systematic calculational procedure. For the free fermion model anticommuting variable correlations are calculated (Sec. V). They are first considered in momentum space where the computations reduce to solving modified miniature dimer problems. The Ising model is included in the free fermion model, so that the results of Sec. V can be used to calculate spin correlations. Section VI exemplifies

this by considering two horizontal spins. The approach generalizes so that one may, in principle, compute the vacuum expectation value of an arbitrary number of spins, although the form of the answer is cumbersome. This is because spin variables, which are the physical variables, are complicated functions of the anticommuting variables, which are the mathematical variables in terms of which computations are simple.

Paper I was a pedagogical introduction to Grassmann integral techniques. It emphasized how to use anticommuting variables and how to express partition functions as fermionic-like field theories. This paper emphasizes computational methods. It illustrates how to calculate partition functions and correlation functions. It provides graphical rules which simplify complicated calculations.

This paper considers only solvable models. They form the testing ground to see how and if the techniques work. They also form a solid foundation upon which unsolved problems may be attacked by approximation methods. The real power of anticommuting variables will come when they are applied to these unsolved models.

II. THE PARTITION FUNCTIONS FOR THE DIMER AND ISING MODELS.

In paper I, the two-dimensional Ising model was represented as a Grassmann integral over a pseudo-free fermionic-like action. A similar representation was obtained for the close-packed dimer problem. By pseudo-free action, I mean a quadratic action. Such theories are solvable by the same methods that solve free theories: transform to momentum space. This partially diagonalizes the problem because of translational invariance. What results is a product of Pfaffians of $4T \times 4T$ dimensional matrices. The variable, T, is the number of

η's and $\eta^\dagger$'s per site. If bilinears occur as $\eta\eta^\dagger$'s the problem simplifies to a product of determinants of $T \times T$ dimensional matrices. This is why it is important that the number of variables per site not be too large.

I will always choose α to range from $-M$ to M and β to range from $-N$ to N, so that there are $(2N+1)$ rows and $(2M+1)$ columns. In the Ising model there are $(2N+1)(2M+1)$ sites, whereas in the dimer problem, there were 4 sites per (α, β) unit so that there are $4(2N+1)(2M+1)$ sites in all.

Going to momentum space means writing

$$\eta^r_{\alpha\beta} = \sum_{s,t} \frac{1}{\sqrt{2M+1}} \frac{1}{\sqrt{2N+1}} \exp\left(\frac{2\pi i\alpha s}{2M+1} + \frac{2\pi i\beta t}{2N+1}\right) a^r_{st} \tag{2.1}$$

$$\eta^{r^+}_{\alpha\beta} = \sum_{s,t} \frac{1}{\sqrt{2M+1}} \frac{1}{\sqrt{2N+1}} \exp\left(\frac{-2\pi i\alpha s}{2M+1} - \frac{2\pi i\beta t}{2N+1}\right) a^{r^\dagger}_{st} \ .$$

In eq. (2.1) a^r_{st} and $a^{r^\dagger}_{st}$ are an equivalent set of anticommuting variables; s ranges from $-M$ to M and β ranges from $-N$ to N. The determinant of this transformation is one. One should think in terms of the correspondence:

$$(\alpha, \beta) \longleftrightarrow (x, y) \ , \tag{2.2}$$

$$\left(\frac{2\pi s}{2M+1}, \frac{2\pi t}{2N+1}\right) \longleftrightarrow (p_x, p_y).$$

The variables s and t are simply momentum variables. Equation (2.1) implies periodic boundary conditions. These conditions will always be chosen, so that one is working on a torus[2]).

Equation (2.1) implies the following useful formulas:

$$\sum_{\alpha\beta} \eta^{q\dagger}_{\alpha\beta}\,\eta^{r}_{\alpha\beta} = \sum_{st} a^{q\dagger}_{st}\,a^{r}_{st} \quad ,$$

$$\begin{aligned}
\sum_{\alpha\beta} \eta^{q\dagger}_{\alpha\beta}\,\eta^{r}_{\alpha+1\beta} &= \sum_{st} a^{q\dagger}_{st}\,a^{r}_{st}\,\exp\left(\frac{2\pi i s}{2M+1}\right), \\
\sum_{\alpha\beta} \eta^{q}_{\alpha\beta}\,\eta^{r\dagger}_{\alpha+1\beta} &= \sum_{st} a^{q}_{st}\,a^{r\dagger}_{st}\,\exp\left(\frac{-2\pi i s}{2M+1}\right), \\
\sum_{\alpha\beta} \eta^{q\dagger}_{\alpha\beta}\,\eta^{r}_{\alpha\beta+1} &= \sum_{st} a^{q\dagger}_{st}\,a^{r}_{st}\,\exp\left(\frac{2\pi i t}{2N+1}\right), \\
\sum_{\alpha\beta} \eta^{q}_{\alpha\beta}\,\eta^{r\dagger}_{\alpha\beta+1} &= \sum_{st} a^{q}_{st}\,a^{r\dagger}_{st}\,\exp\left(\frac{-2\pi i t}{2N+1}\right), \\
\sum_{\alpha\beta} \eta^{q}_{\alpha\beta}\,\eta^{r}_{\alpha\beta} &= \sum_{st} a^{q}_{st}\,a^{r}_{-s-t} \quad , \\
\sum_{\alpha\beta} \eta^{q\dagger}_{\alpha\beta}\,\eta^{r\dagger}_{\alpha\beta} &= \sum_{st} a^{q\dagger}_{st}\,a^{r\dagger}_{-s-t} \quad .
\end{aligned} \tag{2.3}$$

The variables, q and r, refer to the types of anticommuting variables. The "operator" $\exp\left(\frac{2\pi i s}{2M+1}\right)$ is like the quantum mechanical operator $\exp(i\Delta x\, p_x)$ which shifts one unit in the x-direction.

Let us first solve the close-packed dimer problem. The square of the partion function has the representation given by eqs. (I.4.1) and (I. 42). Using eqs. (2.1) and (2.3)

$$Z^2_{\text{dimer}}(z_h, z_v) = \int da\,da^{\dagger}\exp(A),$$

$$A = \sum_{st} A_{st} \quad , \tag{2.4}$$

$$\begin{aligned}
A_{st} = \Bigg[& z_h\left(a^{1}_{st}a^{2\dagger}_{st} + a^{4\dagger}_{st}a^{3}_{st}\right) + z_v\left(a^{2\dagger}_{st}a^{3}_{st} + a^{4\dagger}_{st}a^{1}_{st}\right) \\
& + z_h\left(a^{2\dagger}_{st}a^{1}_{st}\exp\left(\frac{2\pi i s}{2M+1}\right) + a^{3}_{st}a^{4\dagger}_{st}\exp\left(-\frac{2\pi i s}{2M+1}\right)\right) \\
& + z_v\left(a^{1}_{st}a^{4\dagger}_{st}\exp\left(\frac{2\pi i t}{2N+1}\right) + a^{3}_{st}a^{2\dagger}_{st}\exp\left(-\frac{2\pi i t}{2N+1}\right)\right)\Bigg] \\
& + \Big[\text{term with } a^{r}_{st} \text{ and } a^{r\dagger}_{st} \text{ interchanged and exponents conjugated}\Big] \, .
\end{aligned}$$

In going from paper I to eq. (2.4) I have set $z^A_h = z^B_h = z_h$ and $z^A_v = z^B_v = z_v$.

The integrals over each (s,t) can be done individually using eq. (I. 2.6) yielding the determinant of the following martix:

$$M_{st} = \begin{pmatrix} 0 & h_s & 0 & -v_t \\ -h_{-s} & 0 & v_t & 0 \\ 0 & -v_{-t} & 0 & -h_{-s} \\ v_{-t} & 0 & h_s & 0 \end{pmatrix}, \qquad (2.5)$$

with

$$h_s = z_h \left(1 - \exp \frac{2\pi i s}{2M+1}\right), \qquad v_t = z_h \left(1 - \exp \frac{2\pi i t}{2N+1}\right). \qquad (2.6)$$

$$\det M_{st} = (h_s h_{-s} + v_t v_{-t})^2 = \left[(2 - 2\cos\tfrac{2\pi s}{2M+1}) z_h^2 + (2 - 2\tfrac{2\pi t}{2N+1}) z_v^2\right]^2. \qquad (2.7)$$

The total answer is the product of these determinants:

$$Z^2_{\text{dimer}}(z_v, z_h) = \prod_{s=-M}^{M} \prod_{t=-N}^{N} \det M_{st} = \exp\left\{ \sum_{s=-M}^{M} \sum_{t=-N}^{N} \ell n(\det M_{st}) \right\}. \qquad (2.8)$$

The free energy per unit site in the thermodynamic limit, $f \equiv - kT \ell n Z$, becomes

$$-\beta f = \frac{1}{4} \int_{-\pi}^{\pi} \frac{dp_x}{(2\pi)} \int_{-\pi}^{\pi} \frac{dp_y}{(2\pi)} \ell n \left[(2 - 2\cos p_x) z_h^2 + (2 - 2\cos p_y) z_v^2\right], \qquad (2.9)$$

which agrees with the well-known answer[3,4,5,6]). In obtaining eq. (2.9) sums have been replaced by integrals in the standard way and $p_x \equiv \frac{2\pi s}{2M+1}$ and $p_y \equiv \frac{2\pi t}{2N+1}$. Finally the factor of $\frac{1}{4}$ is due to fact that there are $4(2N+1)(2M+1)$ sites.

Now consider the two-dimensional Ising model, which can be related to the partition function for closed polygons (reviewed in Section III of paper I). The corresponding action is given by eq. (I. 4.4). In calculating the partition function, any values of b's and a's satisfying $b_h = \pm 1$, $b_v = \pm 1$, $a_1 a_3 = 1$, $a_2 a_4 = 1$, may be used. For convenience choose $b_h = b_v = 1$, $a_1 = a_3 = 1$, and $a_4 = - a_2 = i$. Equations (I. 4.4), (2.1), and (2.3) result in the action

$$A_{\text{closed polygons}} = \sum_{st} A_{st},$$

$$A_{st} = \Big[z_h a^{h\dagger}_{st} a^{h}_{st} \exp\left(\tfrac{2\pi i s}{2M+1}\right) + z_v a^{v\dagger}_{st} a^{v}_{st} \exp\left(\tfrac{2\pi i t}{2N+1}\right) + a^{h\dagger}_{st} a^{v}_{st} + a^{v\dagger}_{st} a^{h}_{st} + i a^{h\dagger}_{st} a^{v\dagger}_{-s-t} + i a^{v}_{st} a^{h}_{-s-t} + a^{v}_{st} a^{v\dagger}_{st} + a^{h}_{st} a^{h\dagger}_{st} \Big]. \qquad (2.10)$$

The (s,t) variables mix with (-s, -t) variables. Therefore, after doing the integrations, eq. (2.10) will result in a product of Pfaffians of 8×8 dimensional matrices. However, transforming

$$a_{st} \to a^{\dagger}_{st}, \qquad a^{\dagger}_{st} \to -a_{st}, \qquad \begin{pmatrix} s < 0 \\ \text{or} \\ s = 0 \; t < 0 \end{pmatrix} \qquad (2.11)$$

for both horizontal and verical variables, the action, (except for A_{00}) becomes of $aa^{\dagger}$ form (this would not have worked for the choice $a_4 = a_2 = 1$):

$$A_{st} = \Big[h_s a^h_{st} a^{h\dagger}_{st} + v_t a^v_{st} a^{v\dagger}_{st} - a^v_{st} a^{h\dagger}_{st} - a^h_{st} a^{v\dagger}_{st} - i\, a^h_{st} a^{v\dagger}_{-s-t} + i\, a^v_{st} a^{h\dagger}_{-s-t} \Big] , \qquad (2.12)$$

where

$$h_s = 1 - z_h \exp\left(\frac{2\pi i s}{2M+1}\right) , \qquad v_t = 1 - z_v \exp\left(\frac{2\pi i t}{2N+1}\right) . \qquad (2.13)$$

By eq. (I. 2.6) the integration over (s,t) and $(-s,-t)$ variables is the determinant of the following matrix:

$$M_{st} = \begin{pmatrix} h_s & -1 & 0 & -i \\ -1 & v_t & i & 0 \\ 0 & -i & h_{-s} & -1 \\ i & 0 & -1 & v_{-t} \end{pmatrix} \quad (s,t) \neq (0,0) . \qquad (2.14)$$

$$\det M_{st} = h_s h_{-s} v_t v_{-t} - (h_s + h_{-s})(v_t + v_{-t}) + 4$$

$$= (1 + z_h^2)(1 + z_v^2) + 2(1 - z_v^2) z_h \cos\frac{2\pi s}{2M+1} + 2(1 - z_h^2) z_v \cos\frac{2\pi t}{2N+1} . \qquad (2.15)$$

The $(0,0)$ integral must be done separately and gives $-(\det M_{00})^{1/2}$.

I conclude

$$Z_{\text{closed polygon}} = \prod_{st} (\det M_{st})^{1/2} ,$$

$$= \exp\left[\frac{1}{2}\sum_{st} \ell n\, (\det M_{st})\right] ,$$

$$\to \exp\left\{ (2N+1)(2M+1)\left(\frac{1}{2}\right) \int_{-\pi}^{\pi}\frac{dp_x}{2\pi} \int_{-\pi}^{\pi}\frac{dp_y}{2\pi} \right.$$

$$\left. \times\ \ell n \left[(1 + z_h^2)(1 + z_v^2) + 2(1 - z_v^2) z_h \cos p_x + 2(1 - z_h^2) z_v \cos p_y\right]\right\} \qquad (2.16)$$

The exponent, $1/2$, compensates for double counting (s,t) and $(-s,-t)$. In the last step of eq. (2.16) the thermodynamic limit has been taken. The angular integration variables, p_x and p_y, are simply momentum variables. Equations (2.16), (I. 3.7), and (I3.8) [or (I. 3.9)] yield the famous Onsager result[7]) for the free energy per unit site

$$-\beta f_{\text{Ising}} = \frac{1}{2} \int_{-\pi}^{\pi} \frac{dp_x}{2\pi} \int_{-\pi}^{\pi} \frac{dp_y}{2\pi}\, \ell n\, 4 \Big[\cosh 2\beta J_v \cosh 2\beta J_h + \sinh 2\beta J_h \cos p_x + \sinh 2\beta J_v \cos p_y\Big] . \qquad (2.17)$$

III. GRAPHICAL EVALUATION OF PARTITION FUNCTIONS

In this section I will introduce a graphical method to calculate partition functions. Later, it will be extended to correlation

functions. I do this because when the number, T, of variables at a site becomes large, the evaluation of Pfaffians and determinants becomes cumbersome. It is important to have a systematic approach. I will introduce a diagrammatic method which organizes the algebraic computations. For the models dealt with so far, it will seem superfluous; however, when more complicated models are encountered, it will be quite useful. The one danger is the possibility of overlooking a graph.

Consider A_{st} in eq. (2.4). It is like a miniature dimer problem on four sites. The first and second brackets [on the left hand side of eq. (2.4)] correspond respectively to the dimers of figs. 1a and 1b. Together they form the miniature dimer problem of fig. 1c. Figure 2 gives the four possible coverings of fig. 1c and their weights. Overall signs are determined by the rules of fig. (I.8). The sum of these diagrams yields eq. (2.7) as it should.

Let us now solve the generalized closed polygon problem given by (I. 4.4), using the diagrammatic approach. This model is called the free-fermion model[8]). This problem has been solved by expressing the partition function as a product of fermion creation and annihilation operators acting on a vacuum[9]). This is the reason for the name free-fermion. The method of reference 9 is, however, different from the one used here. In particular, anticommuting variables satisfy $\{\eta^r, \eta^{s\dagger}\} = 0$ and cannot be thought of creation and annihilation operators which satisfy $\{\psi^{r\dagger}, \psi^{s\dagger}\} = \delta_{rs}$.

In momentum space the action of eq. (I. 4.4) becomes

$$A_{\text{free fermion}} = \sum_{s,t} \Big[z_h a^{h\dagger}_{st} a^{h}_{st} \exp\Big(\frac{2\pi i s}{2M+1}\Big) + z_v a^{v\dagger}_{st} a^{v}_{st} \exp\Big(\frac{2\pi i t}{2N+1}\Big)$$

$$+ a_1 a^{h\dagger}_{st} a^{v}_{st} + a_3 a^{v\dagger}_{st} a^{h}_{st} + a_2 a^{v\dagger}_{st} a^{h\dagger}_{-s-t} + a_4 a^{v}_{st} a^{h}_{-s-t} \qquad (3.1)$$

$$+ b_h a^{h}_{st} a^{h\dagger}_{st} + b_v a^{v}_{st} a^{v\dagger}_{st} \Big] .$$

If (s,t) and (-s, -t) variables are grouped together, the miniature dimer problem associated with eq. (3.1) is illustrated in fig. 3. There are nine possible coverings as fig. 4 shows. The sum of these is

$$L\Big(\frac{2\pi s}{2M+1}, \frac{2\pi t}{2N+1}\Big) = h_s h_{-s} v_t v_{-t} - a_1 a_3 \big(h_s v_t + h_{-s} v_{-t}\big) \qquad (3.2)$$

$$- a_2 a_4 \big(h_s v_{-t} + h_{-s} v_t\big) + \big(a_1 a_3 + a_2 a_4\big)^2 ,$$

where

$$h_s = b_h - z_h \exp\Big(\frac{2\pi i s}{2M+1}\Big) , \qquad (3.3)$$

$$v_t = b_v - z_v \exp\Big(\frac{2\pi i t}{2N+1}\Big) ,$$

or

$$L\left(\frac{2\pi s}{2M+1}, \frac{2\pi t}{2N+1}\right) = \Bigg[\left(b_h^2 + z_h^2 - 2z_h b_h \cos\frac{2\pi s}{2M+1}\right)\left(b_v^2 + z_v^2 - 2z_v b_v \cos\frac{2\pi t}{2N+1}\right)$$

$$- 2\left(a_1 a_3 + a_2 a_4\right)\left(b_h - z_h \cos\frac{2\pi s}{2M+1}\right)\left(b_v - z_v \cos\frac{2\pi t}{2N+1}\right)$$

$$+ 2\left(a_1 a_3 - a_2 a_4\right) z_h z_v \sin\frac{2\pi s}{2M+1} \sin\frac{2\pi t}{2N+1} \qquad (3.4)$$

$$+ \left(a_1 a_3 + a_2 a_4\right)^2\Bigg] \quad .$$

The partition function is

$$Z_{\text{free fermion}} = \left(\prod_{st} L(s,t)\right)^{1/2} \quad , \qquad (3.5)$$

which becomes in the thermodynamic limit

$$-\beta f_{\text{free fermion}} = \frac{1}{2}\int_{-\pi}^{\pi}\frac{dp_x}{2\pi}\int_{-\pi}^{\pi}\frac{dp_y}{2\pi}\,\ell n\, L(p_x, p_y) \quad , \qquad (3.6)$$

where L is given by eq. (3.4). The factor of $1/2$ is due to double counting of (s,t) and $(-s,-t)$. Equations (3.4) and (3.6) agree with the known result[8,10].

IV. SOLVABLE TWO-DIMENSIONAL DIMER PROBLEMS

This section considers solvable two-dimensional dimer problems. By solvable, I mean solvable by the usual Pfaffian methods[5]. The models will be translated into Grassmann integral form, from which a series of graphical rules will be derived. The treatment used here does not differ from the usual Pfaffian treatment. What is gained is a simple graphical approach which allows one to rapidly solve

a dimer problem. Furthermore, the diagrammatic methods extend to any pseudo-free field theory. This section serves as a pedagogical introduction to graphical methods.

I refer the reader to the standard method of solution[5]. There are two key points:

I. Solvability Condition. A planar dimer problem is solvable if its bonds may be oriented so that every elementary polygon is clockwise odd. Planar means it may be drawn on a piece of paper so that bonds do not cross. The bonds are then given an orientation. The direction is usually denoted by an arrow. A polygon is clockwise odd, if when traversing clockwise, one encounters an odd number of bonds oriented in the opposite direction. An elementary polygon is a non self-intersecting polygon made up of bonds which has no bonds in its interior.

II. The Method of Solution. Fix a standard B configuration which covers the lattice. Each covering (these new ones will be called A coverings) when combined with the B configuration results in a set of closed polygons and isolated dimer pairs, the partition function of which has a Pfaffian representation.

Condition I and Observation II make the problem solvable by Pfaffian methods[5].

For every model satisfying I, the Method of Solution II can be translated into Grassmann integral form: A bond oriented from point, P, to point, Q, upon which on A-dimer may be placed corresponds to a term $\eta_P \eta_Q$ in the action (see fig. 5a). A standard B-bond between P and Q corresponds to a term $\eta_Q^\dagger \eta_P^\dagger$ (see fig. 5b). A-dimer operators are ordered with the graph orientations, whereas

B-dimer operators are ordered oppositely to the graph orientations. The action is schematically of the form

$$A_{\text{dimer}} = \sum_{\text{A-dimers}} z_A \eta\eta + \sum_{\text{B-dimers}} \eta^\dagger \eta^\dagger \quad . \tag{4.1}$$

The Boltzmann factors of A-dimers are z_A, whereas B-dimers have unit Boltzmann factors. It is not hard to see that this action produces the closed polygons and isolated dimer pairs used in the Method of Solution II. The signs are all positive because of Condition I. This may be proved by induction on the length of a polygon and employing Kasteleyn's theorem[11]). Figure 6a illustrates one set of orientations on a square lattice which makes every elementary polygon clockwise odd. Figures 6b and 6c show the A-dimers and a standard B-dimer configuration consisting of horizontal dimers. It is convenient to group the sites in units of four as in fig. (I.5). The corresponding action is

$$\begin{aligned} A_{\text{dimer}} = \sum_{\alpha\beta} \Big[& z_h \eta^1_{\alpha\beta} \eta^2_{\alpha\beta} + z_v \eta^2_{\alpha\beta} \eta^3_{\alpha\beta} + z_h \eta^4_{\alpha\beta} \eta^3_{\alpha\beta} + z_v \eta^4_{\alpha\beta} \eta^1_{\alpha\beta} \\ & + z_h \eta^2_{\alpha\beta} \eta^1_{\alpha+1\beta} + z_h \eta^3_{\alpha\beta} \eta^4_{\alpha+1\beta} + z_v \eta^1_{\alpha\beta+1} \eta^4_{\alpha\beta} + z_v \eta^3_{\alpha\beta} \eta^2_{\alpha\beta+1} \Big] \\ & + \sum_{\alpha\beta} \Big[\eta^{2\dagger}_{\alpha\beta} \eta^{1\dagger}_{\alpha\beta} + \eta^{3\dagger}_{\alpha\beta} \eta^{4\dagger}_{\alpha\beta} \Big] \quad , \end{aligned} \tag{4.2}$$

where the notation is that of Paper I (secs. III and IV). Some dimer problems satisfy

Simplifying Condition C. A graph satisfies Simplifying Condition C if vertices can be grouped into two sets (which I call odd and even) such that no two odd (or even) vertices have a bond in common.

When this condition is satisfied, transform $\eta \to \eta^\dagger$ and $\eta^\dagger \to \eta$ at all even sites. This makes the bilinears in the action of the form $\eta\eta^\dagger$, the partition function becomes a product of determinants rather than Pfaffians, the graphical rules simplify, and calculations are easier to do. Figure 7 shows the rectangular lattice after this transformation.

Graphical Rules When Condition C Holds

or

Rules When Bilinears Are of $\eta\eta^\dagger$ Form

1. Group vertices into repeating units that fill a square array. Use (α,β) to label the units and use $r = 1,2,3, \cdots, T$ to label the different vertices within a unit. Figure (I.5) is an example for the square lattice.

2. Consider one unit, U. There are two kinds of bonds: (a) those which are contained within U and (b) those which go from U to some other unit. Of the latter, [(b)], for every bond which goes from a type r vertex in U to a type q vertex in another unit, there is one bond which goes from a type r vertex in another unit to a type q vertex in U. Thus, they occur in pairs. Half are to be included in U and the others ignored and erased. Figure 8 illustrates this for the square lattice.

3. Keep (a) type bonds as they are. For a (b) type bond which goes from an r in U to a q in another unit, "fold" it back into U, so that it goes from r to q within U (see fig. 9). If q is on "o" located in a unit m horizontal spaces to the right and n spaces upward (m and n may be negative) multiply the bond weight by

$$\exp\,(imp_x + inp_y) \quad . \tag{4.3}$$

If q is an "x" multiply the bond weight by the complex conjugate of eq. (4.3), that is

$$\exp\,(-\,imp_x - inp_y) \quad . \tag{4.4}$$

Figure 9 illustrates this. Figure 10 shows all the weights in the square lattice example after Rule 3 has been carried out.

4. Rules 1 through 3 result in a miniature dimer problem. Solve it by finding all coverings and their weights (see fig. 11 for the square lattice). Call the sum of the diagrams $L(p_x, p_y)$. The free energy per site, f, is

$$-\beta f = \frac{1}{T}\int_{-\pi}^{\pi}\frac{dp_x}{2\pi}\int_{-\pi}^{\pi}\frac{dp_y}{2\pi}\,\ell n\, L(p_x, p_y) \quad . \tag{4.5}$$

The factor of $\frac{1}{T}$ occurs because there are T sites per unit.

Figures 12-15 illustrate the solution for the hexangonal lattice dimer problem. Figure 12 shows the lattice, the bond orientations, the units of eight vertices, and the even and odd sites. The "horizontal" direction is in the x-direction; the "vertical" direction is in the y-direction. Both these directions are also shown in Figure 12 (one must tilt the figure a bit). There are three Boltzmann factors, z_h, z_x, and z_y, corresponding to the three directions in which bonds may point. The Boltzmann factors, the A-dimers, and the standard B-dimer configuration are shown in Figure 13. The folded-over miniature dimer problem is shown in Figure 14. The possible coverings and their values are given in Figure 15. The result is eq. (4.6) with T = 8 and

$$L(p_x, p_y) = \Big[z_h^4 + z_x^4\exp(-2ip_x) + z_y^4\exp(2ip_y) + 2z_h^2z_x^2\exp(-ip_x) + 2z_h^2z_y^2\exp(ip_y) - 2z_x^2z_y^2\exp(ip_y - ip_x)\Big] \quad . \tag{4.6}$$

Graphical Rules When Condition C Fails

or

Rules When Bilinears Are of $\eta\eta$ and $\eta^\dagger\eta^\dagger$ Form

These rules will be exemplified by treating the square lattice dimer problem of eq. (4.2). Although Condition C is satisfied, the simplifying transformation will not be performed. Thus the action will be eq. (4.2) as it stands. Figures 6b and 6c show the A and B dimers.

1. Same as above.

2. Same as above.

3. Draw two copies of U (see fig. 16). Call them U_1 and U_2. For (a) type bonds going from r to q draw two lines: one from r in U_1 to q in U_2 and one from r in U_2 to q in U_1

(see fig. 17). For $\eta\eta$ dimers (i.e. A-dimers) of (b) type originating at an r in U and terminating at a q in another unit, again draw two lines. First draw one from r in U_1 to q in U_2 and multiply its weight by $\exp(-\mathrm{imp}_x - \mathrm{inp}_y)$, then draw one from r in U_2 to q in U_1 and multiply its weight by $\exp(\mathrm{imp}_x + \mathrm{inp}_y)$ (see fig. 18). For $\eta^\dagger\eta^\dagger$ dimers (i.e. B-dimers) do the same as for $\eta\eta$ dimers but multiply weights by the complex conjugated phase factors of the $\eta\eta$ case (see fig. 18). In all cases, if bonds are oriented from r to q they remain so, regardless of whether they go from U_1 to U_2 or U_2 to U_1. Figure 19 shows the resulting weights for the square lattice.

4. Solve the miniature dimer problem (see fig. 20) and call the result $L(p_x, p_y)$. The free energy per unit site is

$$-\beta f = \frac{1}{2T} \int_{-\pi}^{\pi} \frac{dp_x}{2\pi} \int_{-\pi}^{\pi} \frac{dp_y}{2\pi} \ln L(p_x, p_y) \,. \qquad (4.7)$$

Graphical Rules For A General Pseudo-Free Theory

In general, there will be $\eta\eta^\dagger$, $\eta\eta$, and $\eta^\dagger\eta^\dagger$ products. Two copies, U_1 and U_2, of U are to be drawn. Follow the second set of rules, 1,2,3, for $\eta\eta$ and $\eta^\dagger\eta^\dagger$ products. For $\eta\eta^\dagger$ terms use rule 3 of the first set for the U_1 copy of U but for U_2 use complex conjugated phase factors. Finally, use eq. (4.7) and rule 4. Figures 3 and 4 illustrate this for the action given in eq. (I. 4.4).

V. ANTICOMMUTING VARIABLE CORRELATIONS

This section will compute the anticommuting variable correlations (or "propagators") for the free fermion model [eq. (I. 44)]. The configurations and their weights were given in fig. I. 11. In addition, there are z_h and z_v Boltzmann factors for each unit of horizontal and vertical Bloch wall.

The correlation functions will first be calculated in momentum space and then in coordinate space. It will be done graphically. The variables s and t will be used instead of p_x and p_y. The two are related by eq. (2.2).

Consider $\langle a^h_{st} a^{h\dagger}_{st} \rangle$. The operator $a^h_{st} a^{h\dagger}_{st}$ places a dimer between the "o" and "x" at the horizontal (s, t) site. Unlike $\exp(a^h_{st} a^{h\dagger}_{st})$, however, one must use it. Therefore, $Z\langle a^h_{st} a^{h\dagger}_{st} \rangle$ is related to the miniature dimer problem (MDP) of fig. 3, where one inserts a "superbond" and erases all other bonds which connect to the (s,t) horizontal sites. The result is the modified miniature dimer problem (MMDP) of fig. 21(a). To calculate $\langle a^h_{st} a^{h\dagger}_{st} \rangle$ take the value of the MMDP and divide it by the value of the MDP of fig. 3.

General Rules For Calculating Momentum Space Correlation Functions

1. Obtain the MDP using the rules of the last section. Since s and t variables are used rewrite, p_x and p_y in terms of s and t using the correspondence of eq. (2.2). Calculate the value of the MDP and call it $D(s, t) \equiv L(p_x, p_y) = L\left(\frac{2\pi s}{2M+1}, \frac{2\pi t}{2N+1}\right)$.

2. Let a^1 and a^2 denote two generic anticommuting variables in the MDP of rule 1. To calculate $\langle a^1 a^2 \rangle$ draw a superbond from 1 to 2 and assign it unit weight. Erase all bonds involving the 1 and 2 variables. This is the MMDP. Call its value N(s, t). Then

$$\langle a^1 a^2 \rangle = N(s, t) \,/\, D(s, t) \,. \qquad (5.1)$$

Figures 21-24 calculate the non-zero $\langle aa^\dagger \rangle$ free fermion correlations, by showing first the MMDP and then its coverings. In these figures, the upper left and upper right variables are respectively a^v_{st}, $a^{v\dagger}_{st}$, and a^v_{-s-t}, $a^{v\dagger}_{-s-t}$. The lower left and lower right pairs are a^h_{st}, $a^{h\dagger}_{st}$, and a^h_{-s-t}, $a^{h\dagger}_{-s-t}$. The bond weights are those of Figure 3. The superbonds, denoted by darker lines, have unit weight. Figure 25 shows the MMDP's for the $\langle aa^\dagger \rangle$ correlations which have no coverings. They have zero value. Figures 26-28 and Figures 29-31 calculate the non-zero $\langle aa \rangle$ and $\langle a^\dagger a^\dagger \rangle$ correlations. Finally fig. 32 shows the MMDP's for the two remaining correlations which have no coverings. The tabulated results are

$$\langle a^h_{st} a^{h\dagger}_{st} \rangle = (h_{-s} v_t v_{-t} - a_1 a_3 v_t - a_2 a_4 v_{-t}) \,/\, D(s, t) \quad \text{(Fig. 21)}, \quad (5.2)$$

$$\langle a^v_{st} a^{v\dagger}_{st} \rangle = (h_s h_{-s} v_{-t} - a_1 a_3 h_s - a_2 a_4 h_{-s}) \,/\, D(s, t) \quad \text{(Fig. 22)}, \quad (5.3)$$

$$\langle a^h_{st} a^{v\dagger}_{st} \rangle = a_1 \left[h_{-s} v_{-t} - (a_1 a_3 + a_2 a_4) \right] \,/\, D(s, t) \quad \text{(Fig. 23)}, \quad (5.4)$$

$$\langle a^v_{st} a^{h\dagger}_{st} \rangle = a_3 \left[h_{-s} v_{-t} - (a_1 a_3 + a_2 a_4) \right] \,/\, D(s, t) \quad \text{(Fig. 24)}, \quad (5.5)$$

$$\langle a^v_{st} a^{h\dagger}_{-s-t} \rangle = 0 \quad \text{(Fig. 25(a))}, \quad (5.6)$$

$$\langle a^h_{st} a^{v\dagger}_{-s-t} \rangle = 0 \quad \text{(Fig. 25(b))}, \quad (5.7)$$

$$\langle a^h_{st} a^{h\dagger}_{-s-t} \rangle = 0 \quad \text{(Fig. 25(c))}, \quad (5.8)$$

$$\langle a^v_{st} a^{v\dagger}_{-s-t} \rangle = 0 \quad \text{(Fig. 25(d))}, \quad (5.9)$$

$$\langle a^h_{st} a^h_{-s-t} \rangle = a_1 a_2 (v_t - v_{-t}) \,/\, D(s, t) \quad \text{(Fig. 26)}, \quad (5.10)$$

$$\langle a^v_{st} a^v_{-s-t} \rangle = a_2 a_3 (h_{-s} - h_s) \,/\, D(s, t) \quad \text{(Fig. 27)}, \quad (5.11)$$

$$\langle a^v_{st} a^h_{-s-t} \rangle = a_2 \left[(a_1 a_3 + a_2 a_4) - h_s v_{-t} \right] \,/\, D(s, t) \quad \text{(Fig. 28)}, \quad (5.12)$$

$$\langle a^v_{st} a^h_{st} \rangle = 0 \quad \text{(Fig. 32(a))}, \quad (5.13)$$

$$\langle a^{h\dagger}_{st} a^{h\dagger}_{-s-t} \rangle = a_3 a_4 (v_t - v_{-t}) \,/\, D(s, t) \quad \text{(Fig. 29)}, \quad (5.14)$$

$$\langle a^{v\dagger}_{st} a^{v\dagger}_{-s-t} \rangle = a_1 a_4 (h_{-s} - h_s) \,/\, D(s, t) \quad \text{(Fig. 30)}, \quad (5.15)$$

$$\langle a^{v\dagger}_{st} a^{h\dagger}_{-s-t} \rangle = a_4 \left[(a_1 a_3 + a_2 a_4) - h_s v_{-t} \right] \,/\, D(s, t) \quad \text{(Fig. 31)}, \quad (5.16)$$

$$\langle a^{v\dagger}_{st} a^{h\dagger}_{st} \rangle = 0 \quad \text{(Fig. 32(b))}, \quad (5.17)$$

where h_s, v_t, and $D(s, t)$ are given by eqs. (3.3) and (3.4). Of course, correlations involving (s, t) and (s', t') variables vanish if neither $(s, t) \neq (s', t')$ nor $(s, t) = (-s', -t')$.

To obtain coordinate space correlations, use eq. (2.1) to express η's in terms of a's, and then use the results of eqs. (5.3)-(5.18). The thermodynamic limit can be taken and the correlations are

$$\langle \eta^{h}_{\alpha\beta}\eta^{h\dagger}_{\alpha'\beta'}\rangle = \int_{-\pi}^{\pi}\frac{dp_x}{2\pi}\int_{-\pi}^{\pi}\frac{dp_y}{2\pi}\exp\left[i(\alpha-\alpha')p_x + i(\beta-\beta')p_y\right]\times \tag{5.18}$$

$$\left[h(-p_x)v(p_y)v(-p_y) - a_1a_3v(p_y) - a_2a_4v(-p_y)\right] / L(p_x, p_y) ,$$

$$\langle \eta^{v}_{\alpha\beta}\eta^{v\dagger}_{\alpha'\beta'}\rangle = \int_{-\pi}^{\pi}\frac{dp_x}{2\pi}\int_{-\pi}^{\pi}\frac{dp_y}{2\pi}\exp\left[i(\alpha-\alpha')p_x + i(\beta-\beta')p_y\right]\times$$

$$\left[h(p_x)h(-p_x)v(-p_y) - a_1a_3h(p_x) - a_2a_4h(-p_x)\right] / L(p_x, p_y) , \tag{5.19}$$

$$\langle \eta^{h}_{\alpha\beta}\eta^{v\dagger}_{\alpha'\beta'}\rangle = \int_{-\pi}^{\pi}\frac{dp_x}{2\pi}\int_{-\pi}^{\pi}\frac{dp_x}{2\pi}\exp\left[i(\alpha-\alpha')p_x + i(\beta-\beta')p_y\right]\times$$

$$a_1\left[h(-p_x)v(-p_y) - (a_1a_3 + a_2a_4)\right] / L(p_x, p_y) , \tag{5.20}$$

$$\langle \eta^{v}_{\alpha\beta}\eta^{h\dagger}_{\alpha'\beta'}\rangle = \int_{-\pi}^{\pi}\frac{dp_x}{2\pi}\int_{-\pi}^{\pi}\frac{dp_y}{2\pi}\exp\left[i(\alpha-\alpha')p_x + i(\beta-\beta')p_y\right]\times$$

$$a_3\left[h(-p_x)v(-p_y) - (a_1a_3 + a_2a_4)\right] / L(p_x, p_y) , \tag{5.21}$$

$$\langle \eta^{h}_{\alpha\beta}\eta^{h}_{\alpha'\beta'}\rangle = \int_{-\pi}^{\pi}\frac{dp_x}{2\pi}\int_{-\pi}^{\pi}\frac{dp_y}{2\pi}\exp\left[i(\alpha-\alpha')p_x + i(\beta-\beta')p_y\right]\times$$

$$a_1a_2\left[v(p_y) - v(-p_y)\right] / L(p_x, p_y) , \tag{5.22}$$

$$\langle \eta^{v}_{\alpha\beta}\eta^{v}_{\alpha'\beta'}\rangle = \int_{-\pi}^{\pi}\frac{dp_x}{2\pi}\int_{-\pi}^{\pi}\frac{dp_y}{2\pi}\exp\left[i(\alpha-\alpha')p_x + i(\beta-\beta')p_y\right]\times$$

$$a_2a_3\left[h(-p_x) - h(p_x)\right] / L(p_x, p_y) , \tag{5.23}$$

$$\langle \eta^{v}_{\alpha\beta}\eta^{h}_{\alpha'\beta'}\rangle = \int_{-\pi}^{\pi}\frac{dp_y}{2\pi}\int_{-\pi}^{\pi}\frac{dp_y}{2\pi}\exp\left[i(\alpha-\alpha')p_x + i(\beta-\beta')p_y\right]\times$$

$$a_2\left[(a_1a_3 + a_2a_4) - h(p_x)v(-p_y)\right] / L(p_x, p_y) , \tag{5.24}$$

$$\langle \eta^{h\dagger}_{\alpha\beta}\eta^{h\dagger}_{\alpha'\beta'}\rangle = \int_{-\pi}^{\pi}\frac{dp_x}{2\pi}\int_{-\pi}^{\pi}\frac{dp_y}{2\pi}\exp\left[i(\alpha'-\alpha)p_x + i(\beta'-\beta)p_y\right]\times$$

$$a_3a_4\left[v(p_y) - v(-p_y)\right] / L(p_x, p_y) , \tag{5.25}$$

$$\langle \eta^{v\dagger}_{\alpha\beta}\eta^{v\dagger}_{\alpha'\beta'}\rangle = \int_{-\pi}^{\pi}\frac{dp_x}{2\pi}\int_{-\pi}^{\pi}\frac{dp_y}{2\pi}\exp\left[i(\alpha'-\alpha)p_x + i(\beta'-\beta)p_y\right]\times$$

$$a_1a_4\left[h(-p_x) - h(p_x)\right] / L(p_x, p_y) , \tag{5.26}$$

$$\langle \eta^{v\dagger}_{\alpha\beta}\eta^{h\dagger}_{\alpha'\beta'}\rangle = \int_{-\pi}^{\pi}\frac{dp_x}{2\pi}\int_{-\pi}^{\pi}\frac{dp_y}{2\pi}\exp\left[i(\alpha'-\alpha)p_x + i(\beta'-\beta)p_y\right]\times$$

$$a_4\left[(a_1a_3 + a_2a_4) - h(p_x)v(-p_y)\right] / L(p_x, p_y) , \tag{5.27}$$

where

$$h(p_x) = b_h - z_h\exp(ip_x) ,$$

$$v(p_y) = b_v - z_v\exp(ip_y) , \tag{5.28}$$

and L is given by eq. (3.4). Equations (5.18), (5.19), (5.20), (5.21), (5.22), (5.23), (5.24), (5.25), (5.26), and (5.27) are respectively obtained from eqs. (5.2), (5.3), (5.4), (5.5), (5.10), (5.11), (5.12), (5.14), (5.15), and (5.16) by replacing h_s and v_t

by the corresponding momentum valued functions of eq. (5.28). The factors $\exp\left[i(\alpha - \alpha')p_x\right]$ and $\exp\left[i(\beta - \beta')p_y\right]$ in eqs. (5.18) - (5.24) are translation operators. Equations (5.25) - (5.27) have conjugated translation factors because daggered variables are involved.

Equations (5.18) - (5.27) are the coordinate-space anticommuting variable correlation functions for the free fermion model.

VI. THE ISING MODEL CORRELATION FUNCTIONS

This section will calculated the correlation function of two spin variables in the same row. It will be compared to the known result as a check on anticommuting variable techniques. Two horizontal spins are chosen for illustrative purposes only. The approach extends to an arbitrary pair; in fact, the vacuum expectation value of several σ's can be computed. The only drawback is the cumbersome form of the answer: a Pfaffian of (in general) large size. In short, everything you ever wanted to know about the Ising model is expressible as a Pfaffian.

We will need the free fermion anticommuting variable correlations [eqs. (5.18) - (5.27)]. Bond variables will be used, in which case the Ising model is related to the free fermion (or closed - polygon) partition function by eqs. (I. 3.7) and (I. 3.9), when

$$a_1 = a_2 = a_3 = a_4 = b_v = b_h = -1 \,. \tag{6.1}$$

The weights of configurations are given in fig. I.11. These values must be used (as opposed to the less restrictive conditions $a_1a_3 = a_2a_4 = b_v^2 = b_h^2 = 1$) because correlation functions, unlike the the partition function, need not have the same number of a_1 and a_3

type corners, a_2 and a_4 type corners, etc. This is obvious from eqs. (5.18) - (5.27) where correlations are not simply functions of a_1a_3, a_2a_4, etc.

Spin variable correlation functions can be considered as partition functions on a defective lattice[5]). I refer the reader to reference 5, p. 248 - 257. This means that spin correlations are (up to multiplicative constants) the partition functions of Ising models with modified Bloch wall Boltzmann factors along selected paths. For example, $Z_{\text{Ising}}\langle\sigma_{1,0}\sigma_{m+1,0}\rangle$ is z_h^m times the Ising model with the usual z_h and z_v Boltzmann factors for all Bloch walls except for the horizontal ones between (1,0) and (m + 1, 0) where z_h^{-1} is the Boltzmann factor. This defective lattice partition function is obtained by replacing

$$\exp\left(\sum_{\alpha=1}^{m} z_h \eta^{h\dagger}_{\alpha 0}\eta^{h}_{\alpha+1\,0}\right) \quad \text{by} \quad \exp\left[\sum_{\alpha=1}^{m} z_h \eta^{h\dagger}_{\alpha 0}\eta^{h}_{\alpha+1\,0} + \sum_{\alpha=1}^{m}(z_h^{-1}-z_h)\eta^{h\dagger}_{\alpha 0}\eta^{h}_{\alpha+1\,0}\right]$$

$$= \exp\left(\sum_{\alpha=1}^{m} z_h \eta^{h\dagger}_{\alpha 0}\eta^{h}_{\alpha+1\,0}\right) \prod_{\alpha=1}^{m}\left[1 + (z_h^{-1}-z_h)\eta^{h\dagger}_{\alpha 0}\eta^{h}_{\alpha+1\,0}\right] \,, \text{ so that}$$

$$\langle\sigma_{1,0}\eta_{m+1,\,0}\rangle = \left\langle \prod_{\alpha=1}^{m}\left[z_h + (1 - z_h^2)\eta^{h\dagger}_{\alpha 0}\eta^{h}_{\alpha+1\,0}\right]\right\rangle \tag{6.2}$$

Equation (6.2) typifies how spin variable correlations are related to anticommuting variable correlations. Equation (6.2) can be generalized to the case when the left hand side is the vacuum expectation value of several σ's .

For pseudo-free theories, the following formulas are useful:

$$\langle \eta_1 \eta_2 \cdots \eta_m \rangle = \mathrm{Pf}\ M_{ij} \quad (\text{for } m \text{ even}), \tag{6.3}$$

where

$$M_{ij} = \langle \eta_i \eta_j \rangle . \tag{6.4}$$

If $\langle \eta_i \eta_j \rangle = \langle \eta_i^\dagger \eta_j^\dagger \rangle = 0$, then

$$\langle \eta_1^\dagger \eta_1 \eta_2^\dagger \eta_2 \cdots \eta_m^\dagger \eta_m \rangle = \det M_{ij}, \tag{6.5}$$

where

$$M_{ij} = \langle \eta_i^\dagger \eta_j \rangle . \tag{6.6}$$

These formulas are the anologues of Wick's expansion. In eq. (6.3) one sums over all pairings of η's, the sign of which is determined by how many permutations are required to get the η's in paired form.

The vacuum expectation value of an arbitrary product of spins is expressible as a linear combination of anticommuting variable correlations. These vacuum expectation values can be computed using eqs. (5.18) - (5.27) and eq. (6.3). I will demonstrate this for two horizontal spins.

Equations (5.22) and (5.25) imply $\langle \eta^h_{\alpha 0} \eta^h_{\beta 0} \rangle = \langle \eta^{h\dagger}_{\alpha 0} \eta^{h\dagger}_{\beta 0} \rangle = 0$ for all α and β. Apply eq. (6.5) to (6.2). The z_h term of $\left[z_h + (1 - z_h^2) \eta^{h\dagger}_{\alpha 0}\, \eta^h_{\alpha+1\ 0} \right]$ in eq. (6.2) multiplies the same factor as the term in the Wick expansion obtained by contracting

$\eta^{h\dagger}_{\alpha 0}$ with $\eta^h_{\alpha+1\ 0}$. Therefore

$$\langle \sigma_{1,0} \sigma_{m+1,\ 0} \rangle = \det M_{ij}, \tag{6.7}$$

where

$$M_{ij} = z_h \delta_{ij} + (1 - z_h^2) \langle \eta^{h\dagger}_{i0} \eta^h_{j+1\ 0} \rangle \tag{6.8}$$

$$= \int_{-\pi}^{\pi} \frac{dp_x}{2\pi} \int_{-\pi}^{\pi} \frac{dp_y}{2\pi} \exp\left[ip_x (j - i) \right] \tag{6.8}$$

$$\left\{ z_h - (1 - z_h^2) \exp(ip_x) \left[h(-p_x) v(p_y) v(-p_y) - v(p_y) - v(-p_y) \right] \right\} / L(p_x, p_y) .$$

In obtaining eq. (6.8), eq. (5.18) has been used. Equations (6.7) and (6.8) expres's the correlation function of two horizontal spins as a Toeplitz determinant, as is usually done and yields the correct result[4,5].

To calculate the vacuum expectation value of a product of spin variables, proceed analogously. It will be equivalent to an Ising model on a defective lattice. When expressed in terms of anticommuting variables, it will result in an expression of the form

$$\langle \textstyle\prod \sigma\text{'s} \rangle = \langle (c_{12} + d_{12} \eta_1 \eta_2)(c_{34} + d_{34} \eta_3 \eta_4) \cdots (c_{2m-1\,2m} + d_{2m-1\,2m} \eta_{2m-1} \eta_{2m}) \rangle . \tag{6.9}$$

In eq. (6.9) η_i denotes an anticommuting variable such as $\eta^h_{\alpha\beta}$, $\eta^{h\dagger}_{\alpha\beta}$, $\eta^v_{\alpha\beta}$, or $\eta^{v\dagger}_{\alpha\beta}$. The variables $c_{i\,i+1}$ and $d_{i\,i+1}$ are constants determined by the defective lattice. For convenience

write $d_{i\,i+1} = d_i d_{i+1}$; any values of d_i satisfying this will do. Wick's expansion along with eq. (6.3) tells us that eq. (6.9) is

$$\langle \prod \sigma's \rangle = \mathrm{Pf}\ M_{ij} \ , \tag{6.10}$$

where

$$M_{ij} = \begin{cases} d_i d_j \langle \eta_i \eta_j \rangle + \delta_{i+1\ j} c_{i\ i+1}, & i \text{ odd} \\ d_i d_j \langle \eta_i \eta_j \rangle - \delta_{i-1\ j} c_{i-1\ i}, & i \text{ even} \ . \end{cases} \tag{6.11}$$

The $\langle \eta\eta \rangle$ correlations are given in eqs. (5.18) - (5.28).

In principle, all Ising model spin correlations may be calculated using the above method. The reason they result in such cumbersome expressions is the following: The variables which solve The Ising model are the η's . They might be called the mathematical variables because they represent it as a pseudo-free field theory. Correlation functions of anticommuting variables are simple to compute. Contrast this with the spin variables. They are the physical variables. They are, however, complicated functions of the mathematical variables, the η's, which means that spin variable computations result in cumbersome expressions. In conclusion, there are two types of variables, spin variables which have a simple physical interpretation but are mathematically awkward to work with and η variables which do not have as simple a physical interpretation but are easy to work with mathematically.

VII. SUMMARY

Here is a summary of these first two papers. The focus of attention was solvable two-dimensional statistical mechanics models, in particular, the Ising model, the free-fermion model, and the close-packed dimer problems. The partition functions were expressed as integrals over anticommuting variables. In this form they resembled fermionic field theories. The solvable models had quadratic actions, which were computed by using free field theory techniques. More importantly, a series of graphical rules were derived which allowed one to compute partition functions and anticommuting variable correlation functions by solving miniature dimer problems. This provided a quick and simple graphical calculational approach. Many models can be solved by drawing a few diagrams. Finally, I showed how to calculate the vacuum expectation value of an arbitrary number of Ising spin variables.

For the most part, there are no new results. What has been gained is a powerful reorganization of old methods. Abstruse Pfaffian techniques have been rewritten as a set of simple graphical rules so that calculations are straightforward and systematic. The Grassmann integral has formulated the problem in terms of a field theory where powerful field theory methods have been applied.

These first two papers have dealt with solvable models. One need only add a term,

$$\sum_{\alpha\beta} \Delta \eta^h_{\alpha\beta} \eta^{h\dagger}_{\alpha\beta} \eta^v_{\alpha\beta} \eta^{v\dagger}_{\alpha\beta} \ , \tag{7.1}$$

to the free-fermion action of eq. (I. 4.4) to break the free-fermion constraint and obtain the general eight vertex model[8]). This model is unsolved. It is an interacting field theory. The approximation methods used for interacting field theories can be applied to it. Here is where the real power of anticommuting variables is. Most interesting statistical mechanics problems are not solvable; an example is the 3-d Ising model[12]). It is important to have viable approximation schemes. Such schemes will be obtained via Grassmann integrals. Furthermore, they will be, in general, systematic and simple.

In short, these first two papers have formed a testing ground for anticommuting variable techniques. They formed a solid foundation of solvable models upon which unsolvable models can be approached.

ACKNOWLEDGMENTS

I thank Korkut Bardakci and Harry Morrison for encouragement. I thank Harry Morrison for reading the manuscript and making useful suggestions.

REFERENCES

1. S. Samuel, The Use of Anticommuting Integrals in Statistical Mechanics I. References to equations and figures in this paper will be prefixed by a I, e.g. eq. (I. 1.1) and fig. I.1 refer to equation (1.1) and fig. 1 of reference 1.
2. When this is done, some terms have the incorrect sign (those involving loops around the torus). This difficulty can be overcome by standard methods (see pages 61 to 67 of reference 4). However, in the thermodynamic limit, such configurations will be a zero measure effect and can be ignored.
3. H. N. V. Temperley and M. E. Fisher, Phil. Mag. 6, (1961) 1061. M. E. Fisher, Phys. Rev. 124, (1961) 1664.
4. See, for example, B. M. McCoy and T. T. Wu, The Two-Dimensional Ising Model (Harvard University Press, Cambridge, 1973).
5. See, for example, E. W. Montroll, Brandeis University Summer Institute in Theoretical Physics, 1966, edited by M. Chrétien, E. P. Gross, and S. Deser (Gordon and Breach, New York, 1968).
6. See, for example, H. S. Green and C. A. Hurst, Order-Disorder Phenomena (Interscience, New York, 1964).
7. L. Onsager, Phys. Rev. 65, (1964) 117. Textbook derivations are given in references 4,5, and 6.
8. C. Fan and F. Y. Wu, Phys. Rev. B2, (1970) 723.
9. See reference 6, Chapter 4.
10. Reference 6, Sec. 5.3.
11. P. M. Kasteleyn, J. Math. Phys. 4, (1963) 287. A pedagogical version is given in reference 5.
12. The techniques used here extend to drawing closed surfaces in three

dimensions. Thus, the 3-d Ising model has an interesting interacting fermionic-like field theory representation.

S. Samuel, to be published.

Figure 1. The Miniature Dimer Problem. Figures (a) and (b) are the graphical representation of the first and second terms in A_{st} of eq. (2.4). The h_s, v_t, etc. (eq. 2.6) factors are the weights of the dimers. The sum of (a) and (b) form the miniature dimer problem of (c).

Figure 2. The Four Possible Coverings. The weights of these diagrams are: (a) $(v_t v_{-t})^2$, (b) $(h_s h_{-s})^2$, (c) $(h_s h_{-s} v_t v_{-t})$, (d) $(h_s h_{-s} v_t v_{-t})$. The sum yields eq. (2.7).

Figure 3. The Miniature Dimer Problem for the Free-Fermion model. The upper left "o" and "x" are a^v_{st}, $a^{v\dagger}_{st}$; the lower left are a^h_{st}, $a^{h\dagger}_{st}$; the upper right are a^v_{-s-t}, $a^{v\dagger}_{-s-t}$; the lower right are a^h_{-s-t}, $a^{h\dagger}_{-s-t}$. The weights of bonds are as indicated with h_s and v_t given by eq. (3.3).

Figure 4. The Possible Coverings of fig.3. The arrows are shown to aid in determining the sign [use rules of fig. (I.8)]. The values of there diagrams are (a) $(h_s h_{-s} v_t v_{-t})$, (b) $(- a_1 a_3 h_s v_t)$, (c) $(- a_1 a_3 h_{-s} v_{-t})$, (d) $(a_1 a_3 a_1 a_3)$, (e) $(- a_2 a_4 h_s v_{-t})$, (f) $(- a_2 a_4 h_{-s} v_t)$, (g) $(a_1 a_2 a_3 a_4)$, (h) $(a_1 a_2 a_3 a_4)$, and (i) $(a_2 a_4 a_2 a_4)$.

Figure 5. The A and B Dimer Operators. In (a) is a typical bond oriented from P to Q. In the action will correspond the term $\eta_P \eta_Q$ as in (b). If a standard B-dimer lies on this bond then there is a term $\eta^\dagger_Q \eta^\dagger_P$ as in (c). The A-dimers are associated with $\eta\eta$ products, whereas

B-dimers are associated with $\eta^\dagger \eta^\dagger$ products.

Figure 6. Square Lattice Dimer Problem. Figure (a) shows the orientations which make every elementary square clockwise odd. Figure (b) represents the A-dimer operators and fig. (c) is the standard B-dimer configuration consisting of horizontal dimers.

Figure 7. The Simplifying Transformation. Condition C holds for the square lattice of fig. 6. After the transformation $\eta^\dagger \to \eta$ at even sites, the dimer operators of figs. 6a and 6b become those shown here. The B-dimers are drawn above the A-dimers.

Figure 8. Illustration of Rule 2. Figure (a) shows the (α, β) unit. There are two B-dimers and four A-dimers entirely contained in (α, β). There are eight A-dimers which connect sites in (α, β) to sites in nearby units. They occur in pairs. For example, the upper right A-dimer, $\eta^3_{\alpha\beta} \eta^{2\dagger}_{\alpha\beta+1}$, has a partner, the lower right A-dimer, $\eta^3_{\alpha\beta-1} \eta^{2\dagger}_{\alpha\beta}$. Rule 2 erases one bond from each pair. Figure (b) is an example of what results.

Figure 9. Rule 3 for $\eta\eta^\dagger$ Products. Figure (a) shows the two dimers of fig. 8b which start in the (α, β) unit at sites 2 and 3 and go to the sites 1 and 4 of the $(\alpha + 1, \beta)$ unit. Rule 3 says to "fold" these back into the (α, β) unit as shown in (b). Let "o" and "x" correspond to the anticommuting variables a and $a^\dagger$. Then the $a^\dagger_2 a_1$ bond weight gets multiplied by $\exp(ip_x)$ whereas the $a_3 a^\dagger_4$ weight gets multiplied by $\exp(-ip_x)$.

Figure 10. The Weights for the Square Lattice. Rule 3 applied to fig. 8b results in this figure. The weights of the B-dimers remains 1 as indicated. The A-dimer weights have contributions from (a) type bonds as well as (b) types. When added they result in the factors $h(p_x) = z_h[1 - \exp(ip_x)]$, $v(p_y) = z_v[1 - \exp(ip_y)]$, etc.

Figure 11. The Two Coverings of Figure 10. The value of (a) is $h(p_x)h(-p_x) = z_h^2(2 - 2\cos p_x)$. The value of (b) is $v(p_y)v(-p_y) = z_v^2(2 - 2\cos p_y)$. The sum of these is $L(p_x, p_y)$. When put into eq. (4.5), the free energy per site is obtained.

Figure 12. The Hexagonal Dimer Problem. This is the hexagonal lattice. The above bond orientations make every elementary hexagon clockwise odd. The units are outlined by dotted lines. There are eight sites in each, and (α, β) label them. This lattice satisfies Simplifying Condition C; the odd sites are denoted by larger dots. The x-direction is northeast and the y-direction is northwest as indicated.

Figure 13. The Dimer Operators. Figure (a) shows the A-dimers and their weights. Only half of the "external" dimers have been kept in accord with rule 3. Figure (b) shows the B-dimers. Their weights are unity. If this B configuration is chosen in every unit, then every site is covered by a B-dimer.

Figure 14. The Miniature Dimer Problem. Rule 3 applied to Figure 13 results in this miniature dimer problem with the indicated bond weights.

Figure 15. The Coverings of Figure 14. There are nine coverings. Their values are (a) (z_h^4), (b) $\left(z_x^4 \exp(-2ip_x)\right)$, (c) $\left(z_y^4 \exp(2ip_y)\right)$, (d) $\left(z_h^2 z_x^2 \exp(-ip_x)\right)$, (e) $\left(z_h^2 z_x^2 \exp(-ip_x)\right)$, (f) $\left(z_h^2 z_y^2 \exp(ip_y)\right)$, (g) $\left(z_h^2 z_y^2 \exp(ip_y)\right)$, (h) $\left(-z_x^2 z_y^2 \exp(ip_y - ip_x)\right)$ and (i) $\left(-z_x^2 z_y^2 \exp(ip_y - ip_x)\right)$. The sum of these values gives the $L(p_x, p_y)$ of eq. (4.6).

Figure 16. The Two Copies. For the square lattice, U consists of four sites. Rule 3 says to draw two copies of U. These are labelled U_1 and U_2. The different sites within each U_1 have been numbered 1,2,3, and 4. One should think of U_1 as representing (s, t) variables and U_2 as representing (-s, -t) variables.

Figure 17. The (a)-Type Bonds. In Figure (a), there is an A-dimer from fig. 6b and a B-dimer from fig. 6c. Each of these results in two dimers, one from U_1 to U_2 and one from U_2 to U_1 as (b) indicates. The orientation remains the same, so that the A-dimer in U which goes from 4 to 3, still goes from 4 to 3 in both cases in Figure (b).

Figure 18. The (b)-type Bonds. Figure (a) shows one $\eta\eta$ (b)-type bond and one $\eta^\dagger\eta^\dagger$ (b)-type bond. Although the latter does not occur in the standard B configuration of

fig. 6c, it has been put in here for illustrative purposes. If U is the (α, β) unit then the two bonds go from the (α, β) unit to the $(\alpha + 1, \beta)$ unit. Both give rise to two dimers in (b) the weights of which get multiplied by the indicated phase factors.

Figure 19. The Resulting Bond Weights. Figure (a) shows the resulting A-dimers and their bond weights. Figure (b) shows the B-dimers. Their weights are all unity. Here, $h(p_x) = z_h[1 - \exp(ip_x)]$ and $v(p_y) = z_v[1 - \exp(ip_y)]$. When superimposed (a) and (b) give rise to a miniature dimer problem.

Figure 20. The Coverings of Figure 19. There are four coverings of Figure 19. Their values are (a) $[h(p_x)h(-p_x)]^2$, (b) $[v(p_y)v(-p_y)]^2$, (c) $[h(p_x)h(-p_x)v(p_y)v(-p_y)]$, and (d) $[h(p_x)h(-p_x)v(p_y)v(-p_y)]$.

Figure 21. The $\langle a^h_{st} a^{h\dagger}_{st} \rangle$ correlation. Figure (a) is the MMDP. Figures (b), (c), and (d) are the coverings. Their values are (b) $(h_{-s} v_t v_{-t})$, (c) $(-a_1 a_3 v_t)$, and (d) $(-a_2 a_4 v_{-t})$.

Figure 22. The $\langle a^v_{st} a^{v\dagger}_{st} \rangle$ correlation. Figure (a) is the MMDP. Figures (b), (c), and (d) are the coverings. Their values are (b) $(h_s h_{-s} v_{-t})$, (c) $(-a_1 a_3 h_s)$, and (d) $(-a_2 a_4 h_{-s})$.

Figure 23. The $\langle a^h_{st} a^{v\dagger}_{st} \rangle$ correlation. Figure (a) is the MMDP. Figures (b), (c) and (d) are the coverings. Their values are (b) $(-a_1 a_2 a_4)$, (c) $(-a_1 a_1 a_3)$, and (d) $(a_1 h_{-s} v_{-t})$.

Figure 24. The $\langle a^v_{st} a^{h\dagger}_{st} \rangle$ correlation. Figure (a) is the MMDP. Figures (b), (c), and (d) are the coverings. Their values are (b) $(-a_2 a_3 a_4)$, (c) $(-a_1 a_3 a_3)$, and (d) $(a_3 h_{-s} v_{-t})$.

Figure 25. The zero $\langle aa^\dagger \rangle$ correlations. Figures (a), (b), (c), and (d) are the MMDP's for the $\langle a^v_{st} a^{h\dagger}_{-s-t} \rangle$, $\langle a^h_{st} a^{v\dagger}_{-s-t} \rangle$, $\langle a^h_{st} a^{h\dagger}_{-s-t} \rangle$, and $\langle a^v_{st} a^{v\dagger}_{-s-t} \rangle$ correlations. None of these MMDP's have any coverings.

Figure 26. The $\langle a^h_{st} a^h_{-s-t} \rangle$ correlations. Figure (a) is the MMDP. Figures (b) and (c) are the two coverings. Their values are (b) $(a_1 a_2 v_t)$ and (c) $(-a_1 a_2 v_{-t})$.

Figure 27. The $\langle a^v_{st} a^v_{-s-t} \rangle$ correlation. Figure (a) is the MMDP. Figures (b) and (c) are the two coverings. Their values are (b) $(-a_2 a_3 h_s)$ and (c) $(a_2 a_3 h_{-s})$.

Figure 28. The $\langle a^v_{st} a^h_{-s-t} \rangle$ correlation. Figure (a) is the MMDP. Figures (b), (c), and (d) are the coverings. Their values are (b) $(a_2 a_2 a_4)$, (c) $(a_1 a_2 a_3)$, and (d) $(-a_2 h_s v_{-t})$.

Figure 29. The $\langle a^{h\dagger}_{st} a^{h\dagger}_{-s-t} \rangle$ correlations. Figure (a) is the MMDP. Figures (b) and (c) are the coverings. Their values are (b) $(a_3 a_4 v_t)$ and (c) $(-a_3 a_4 v_{-t})$.

Figure 30. The $\langle a^{v\dagger}_{st} a^{v\dagger}_{-s-t} \rangle$ correlation. Figure (a) is the MMDP. Figures (b) and (c) are the coverings. Their values are (b) $(a_1 a_4 h_{-s})$ and (c) $(-a_1 a_4 h_s)$.

Figure 31. The $\langle a^{v\dagger}_{st} a^{h\dagger}_{-s-t} \rangle$ correlation. Figure (a) is the MMDP. Figures (b), (c), and, (d) are the coverings. Their values are (b) $(a_2 a_4 a_4)$, (c) $(a_1 a_3 a_4)$, and (d) $(-a_4 h_s v_{-t})$.

Figure 32. The $\langle a^v_{st} a^h_{st} \rangle$ and $\langle a^{v\dagger}_{st} a^{h\dagger}_{st} \rangle$ correlations. Figures (a) and (b) are the MMDP's. Neither has a covering

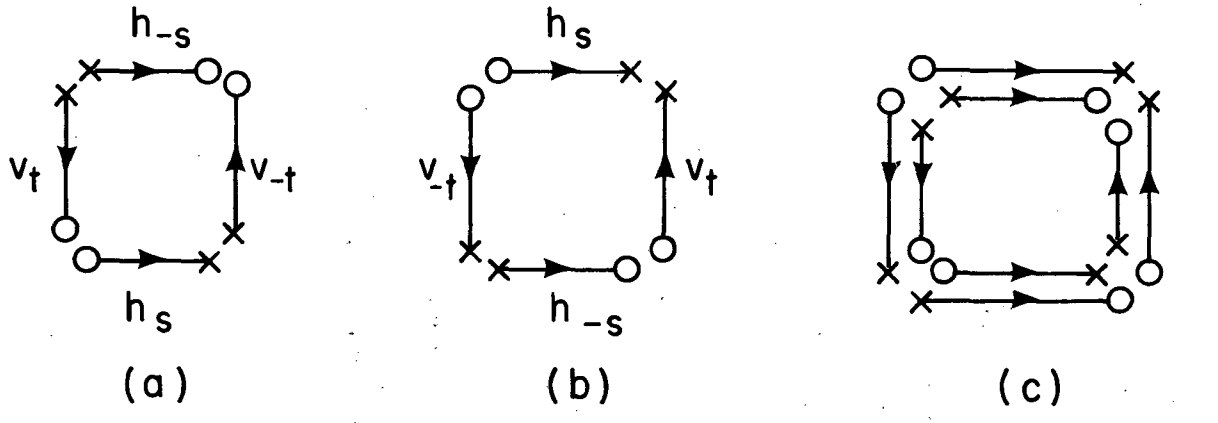

Figure 1

XBL7810-11589

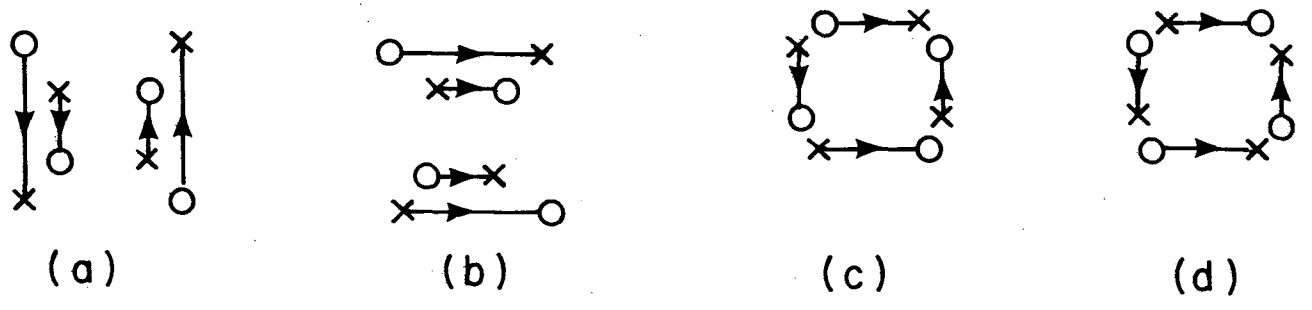

Figure 2

XBL7810-11590

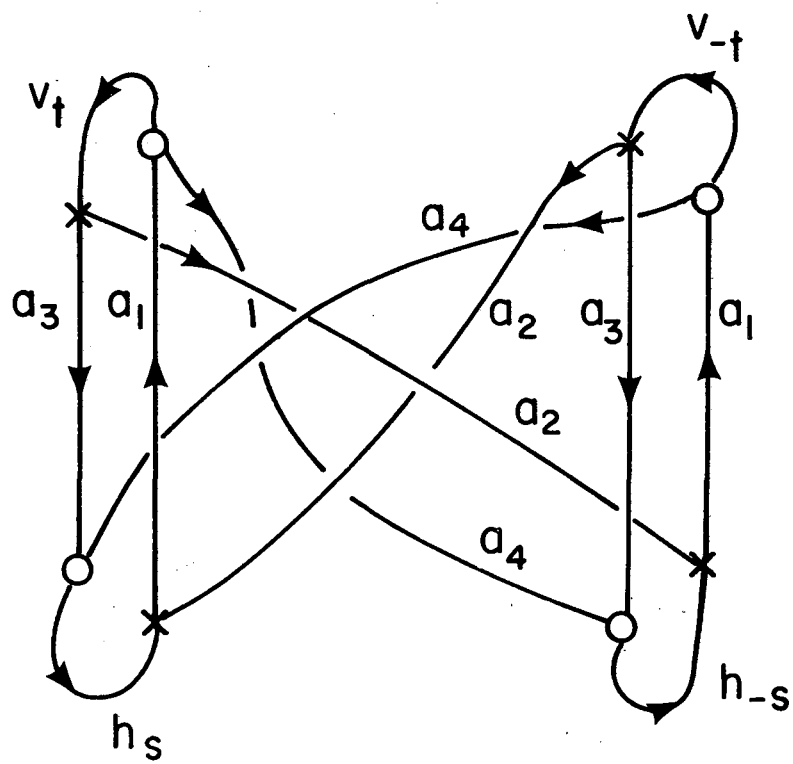

Figure 3 XBL 7810-11598

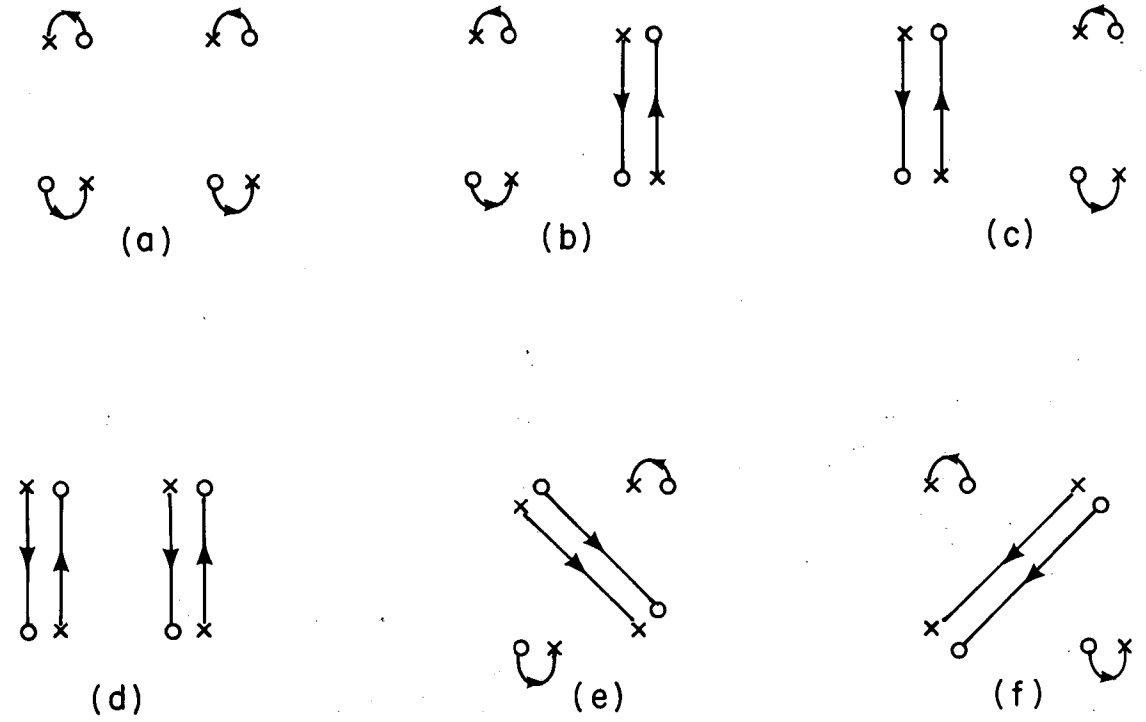

Figure 4

XBL7810 - 6608

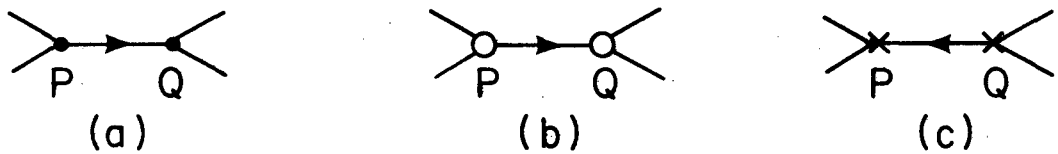

Figure 5

XBL7810-11593

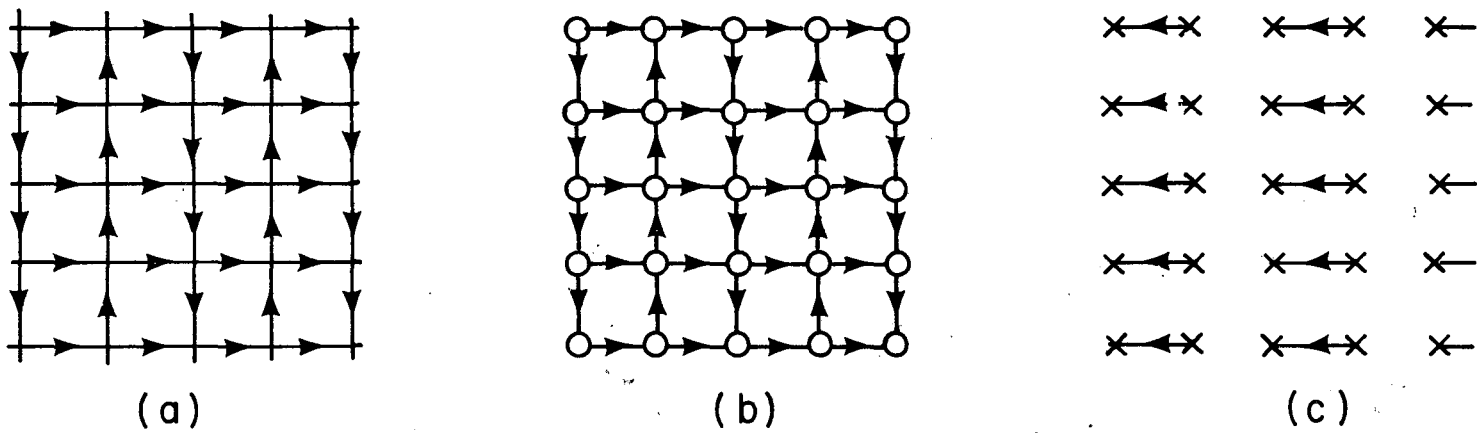

Figure 6

XBL7810-11594

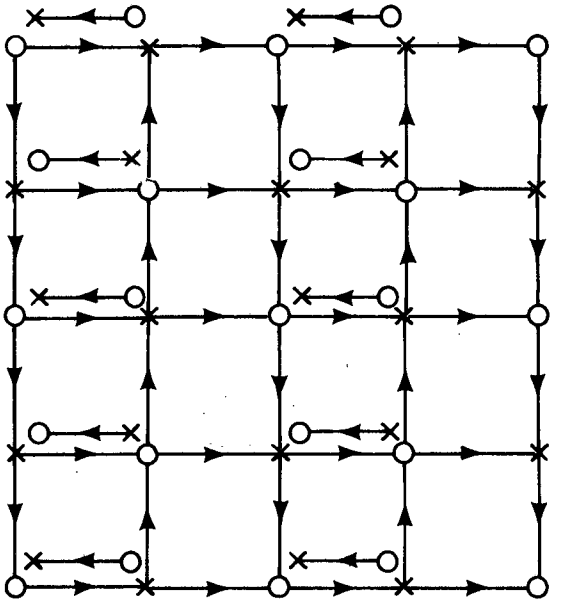

Figure 7 XBL7810-11591

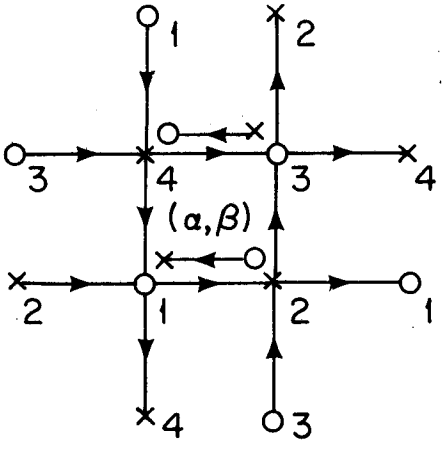

(a)

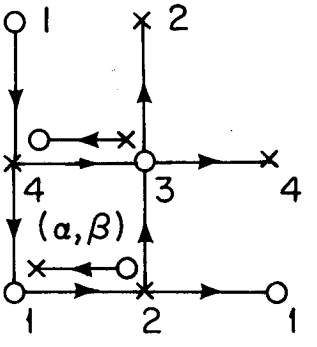

(b)

Figure 8 XBL7810-11592

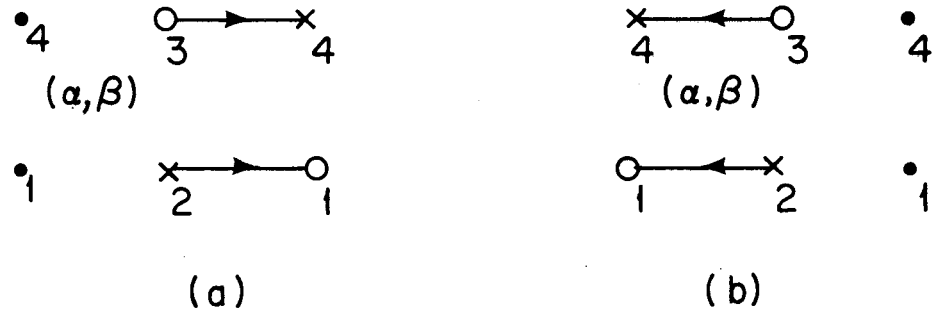

Figure 9 XBL7810-11581

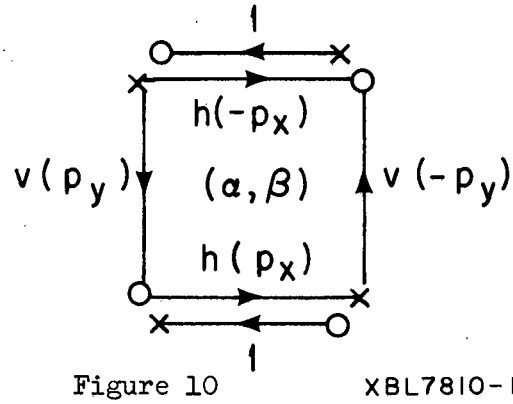

Figure 10 XBL7810-11582

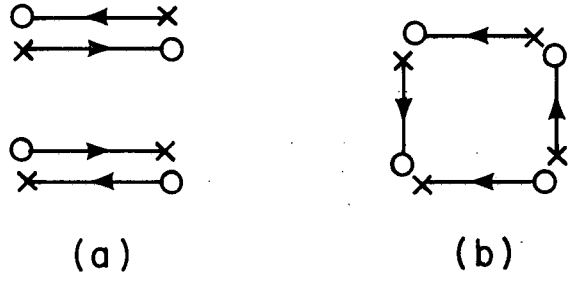

Figure 11 XBL7810-11583

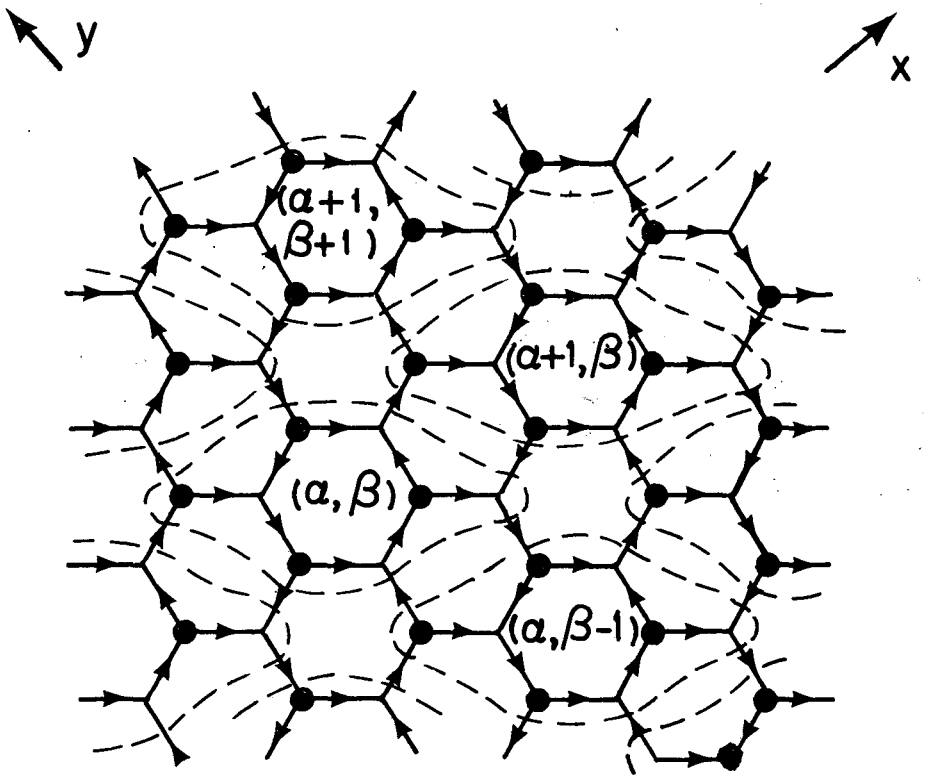

Figure 12 XBL7810-6620

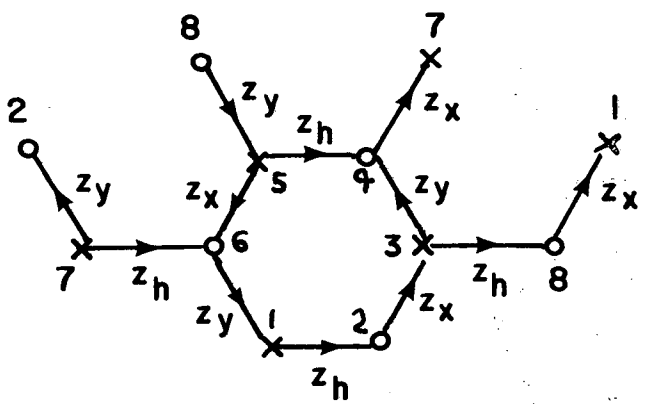

(a)

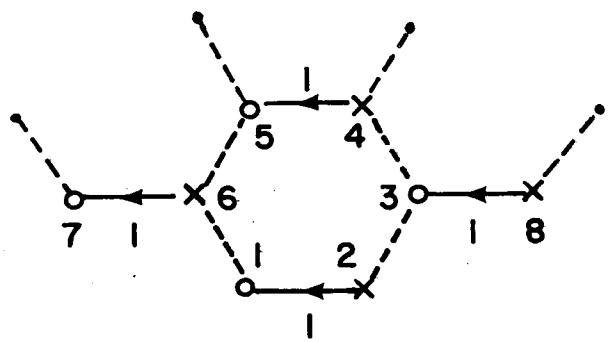

(b)

Figure 13

XBL7810-6619

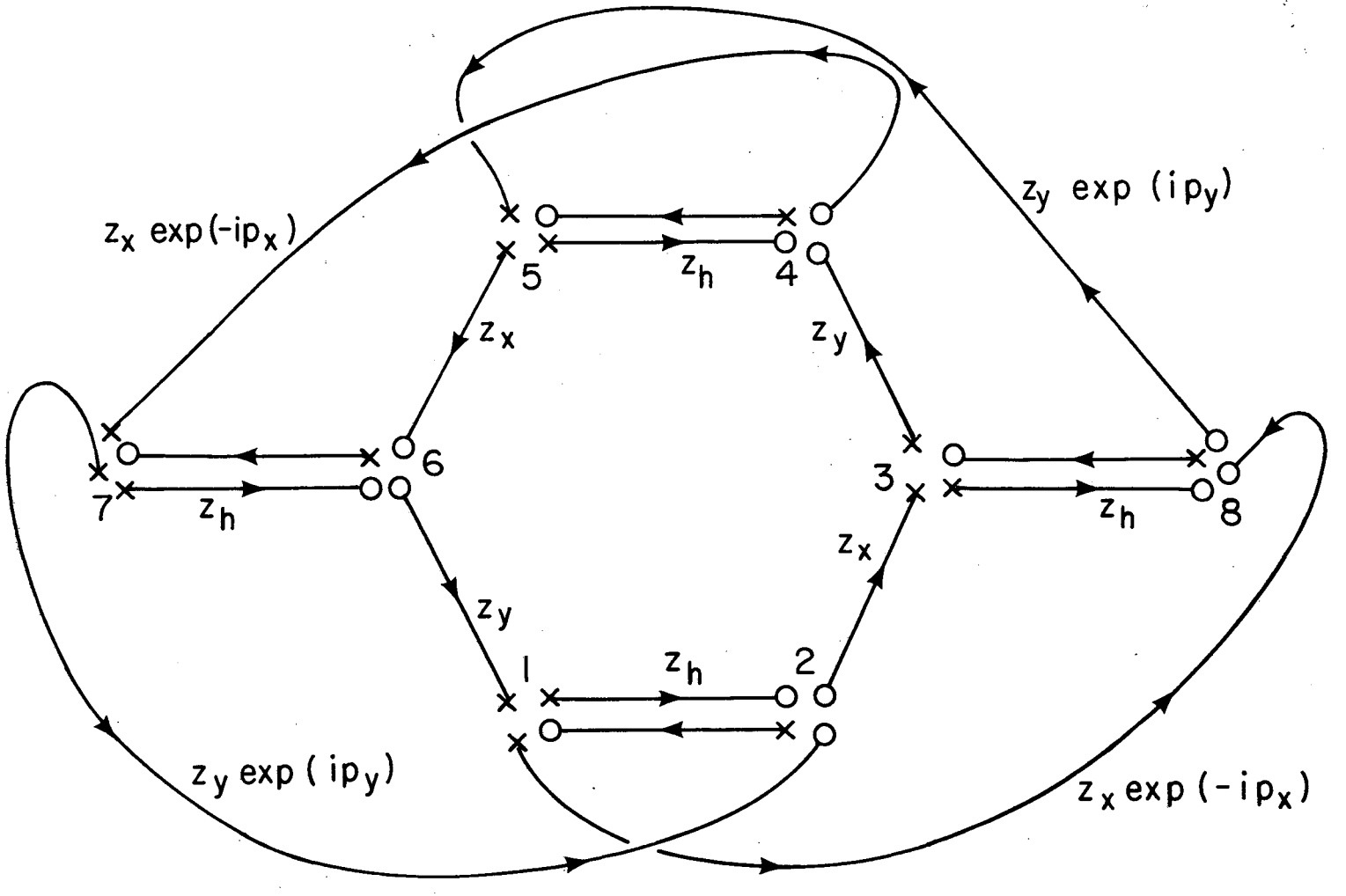

Figure 14

XBL7810-11588

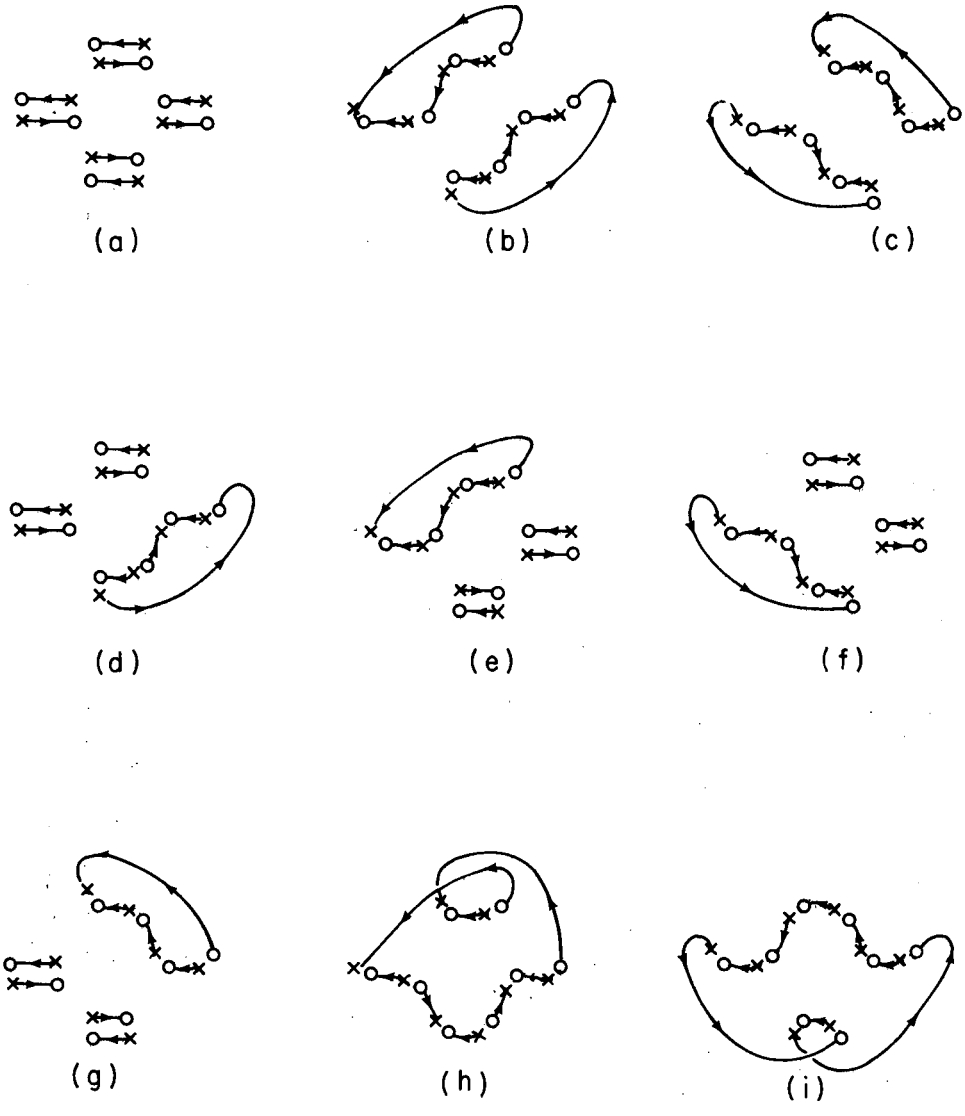

Figure 15

XBL7810-11584

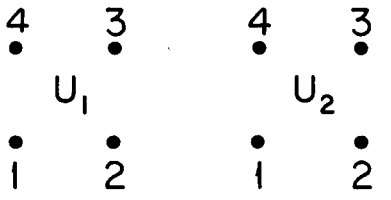

Figure 16 XBL7810-11595

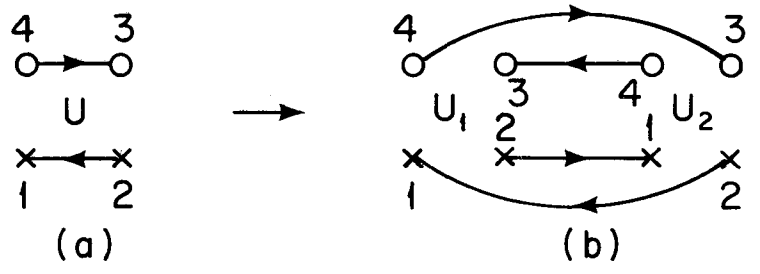

Figure 17 XBL7810-11596

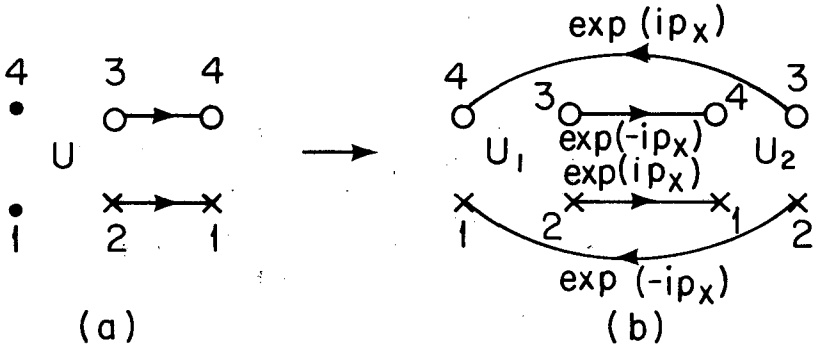

Figure 18 XBL7910-11597

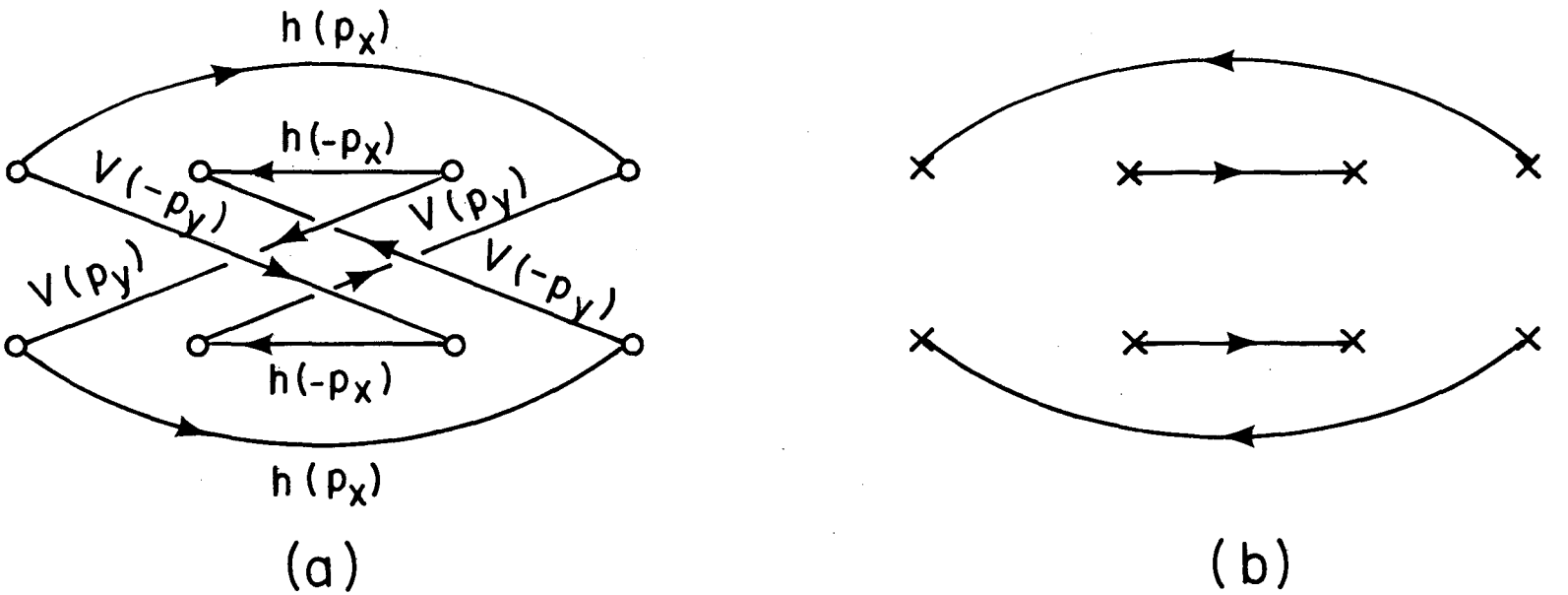

Figure 19

XBL7810-6618

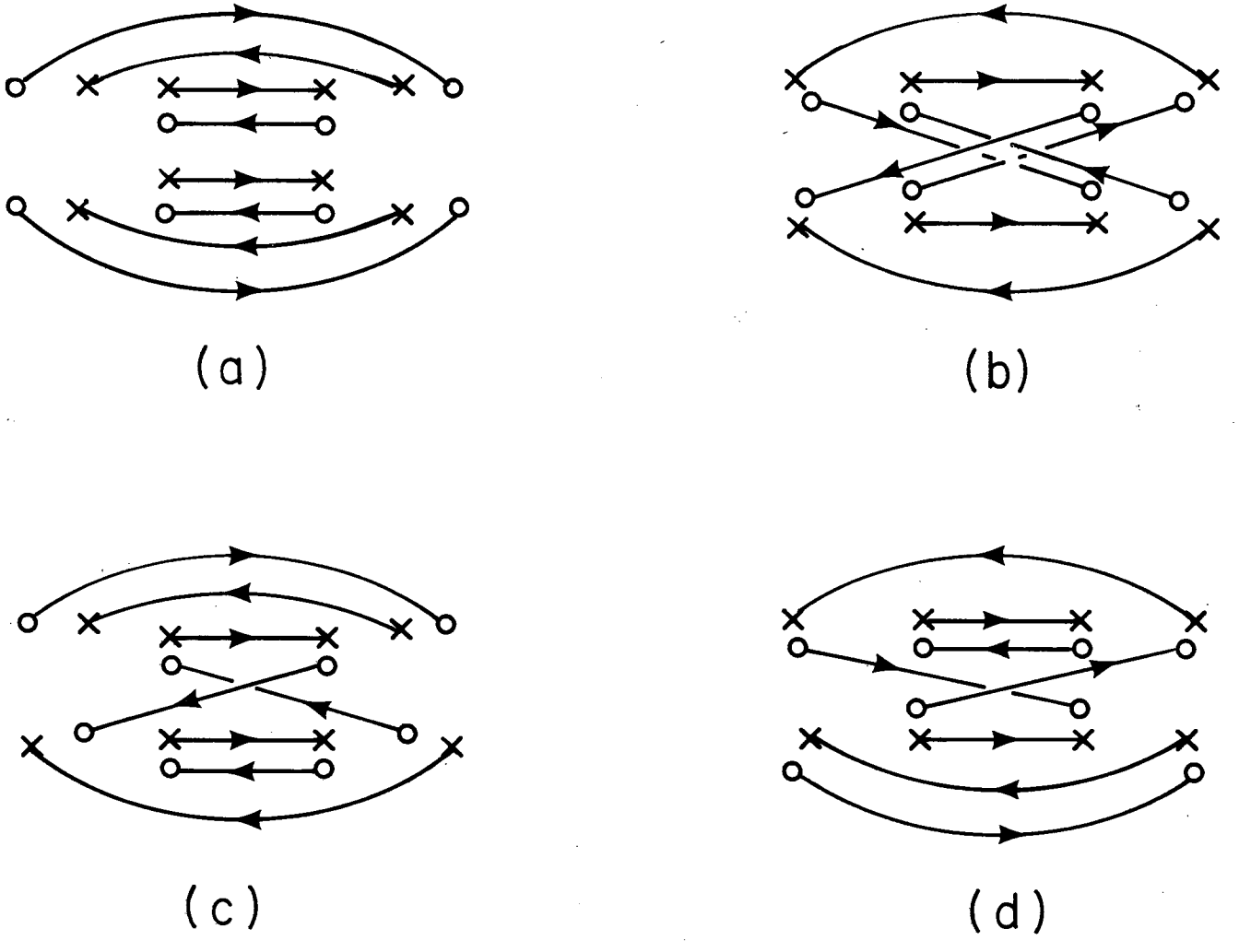

Figure 20

XBL7810-6617

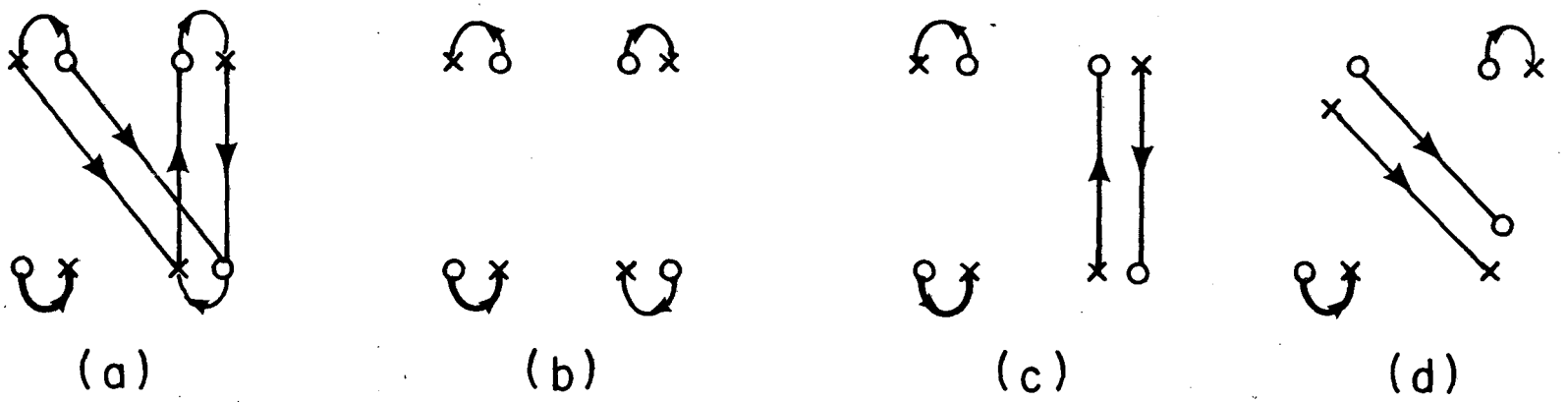

Figure 21

XBL7810-6611

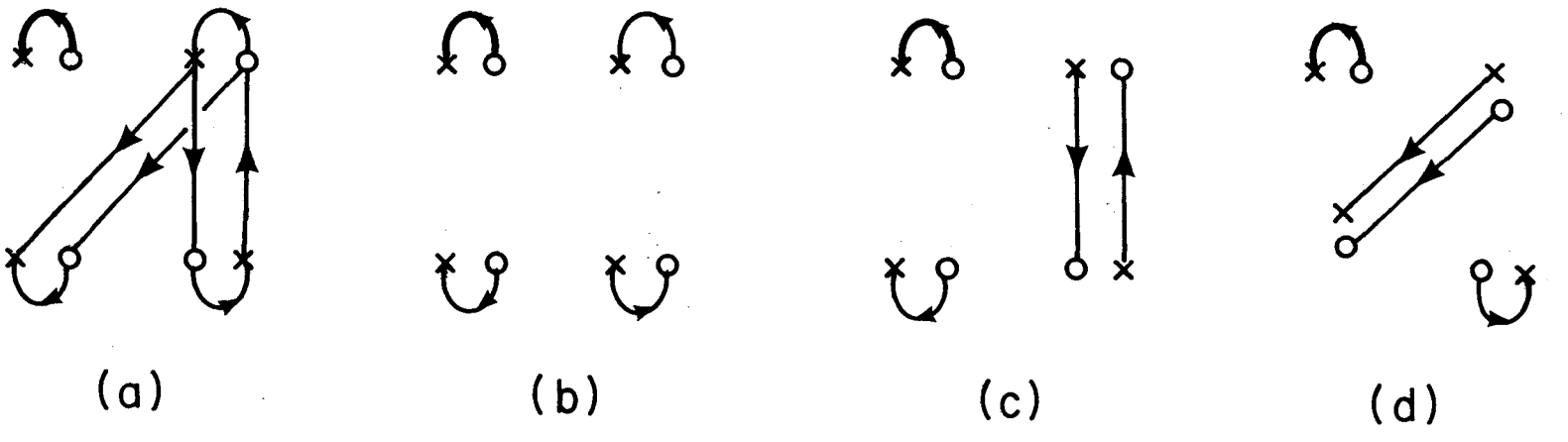

Figure 22

XBL7810-6610

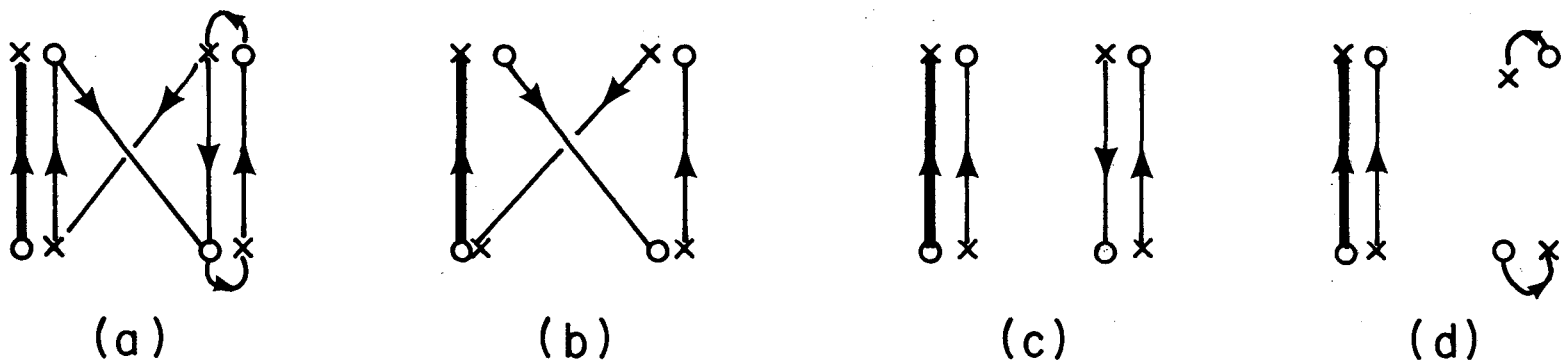

Figure 23

XBL 7810-6609

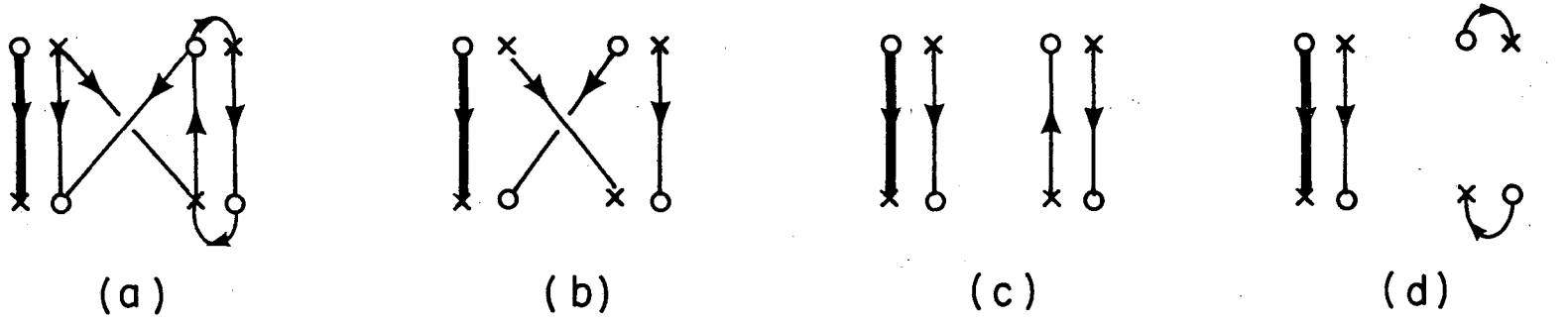

Figure 24

XBL7810-6613

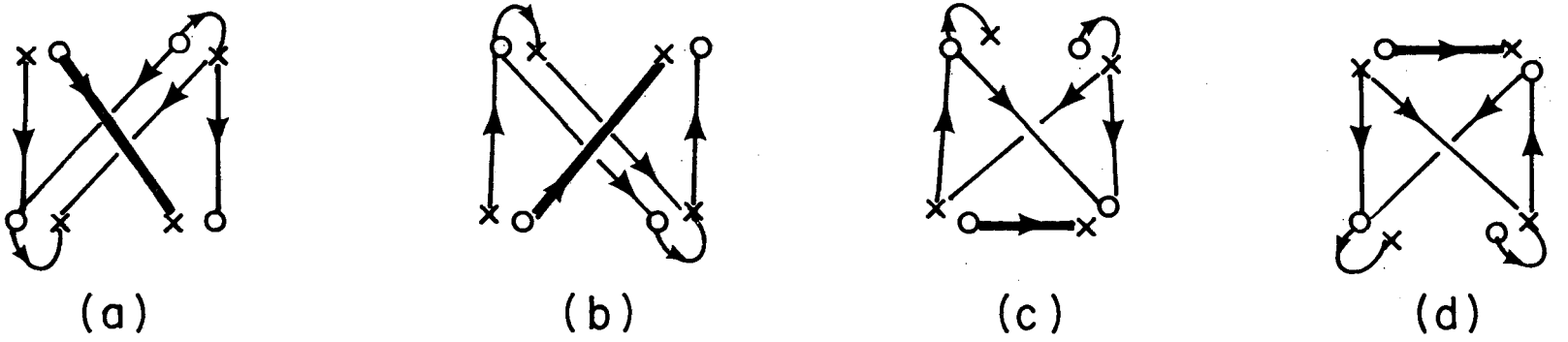

Figure 25

XBL7810-6616

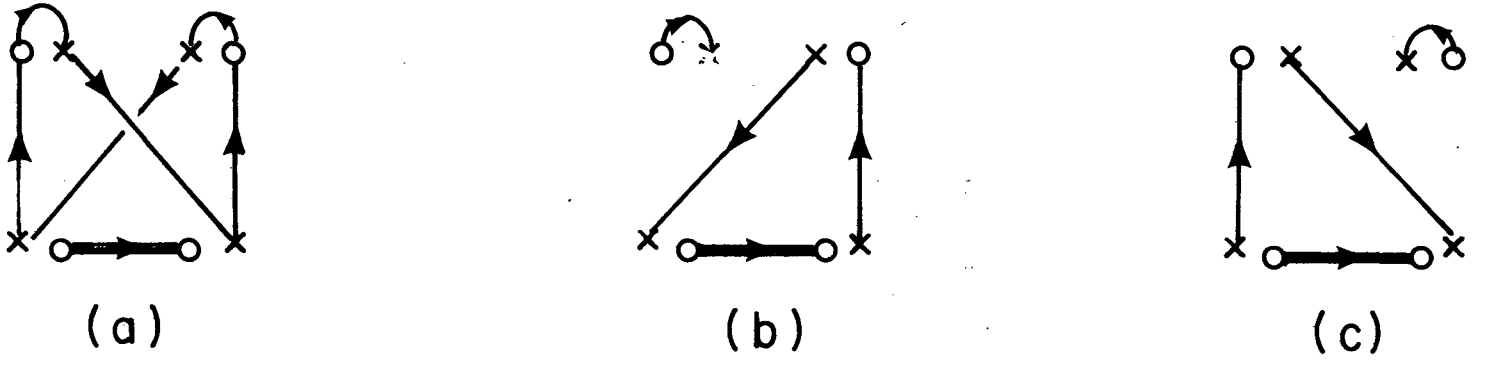

Figure 26

XBL7810-6621

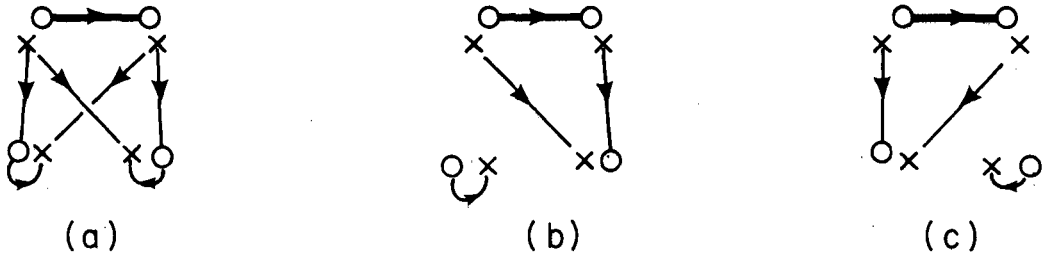

Figure 27

XBL7810 - 11585

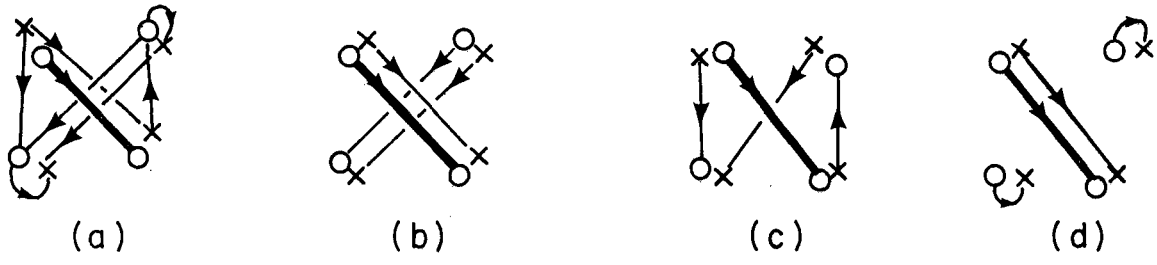

Figure 28

XBL7810 - 11586

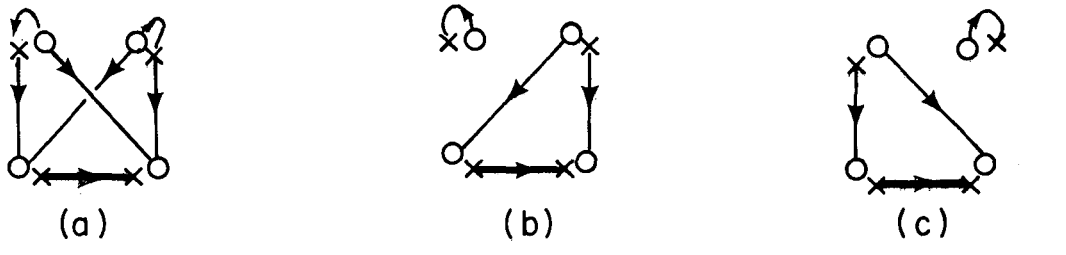

Figure 29

XBL7810-11587

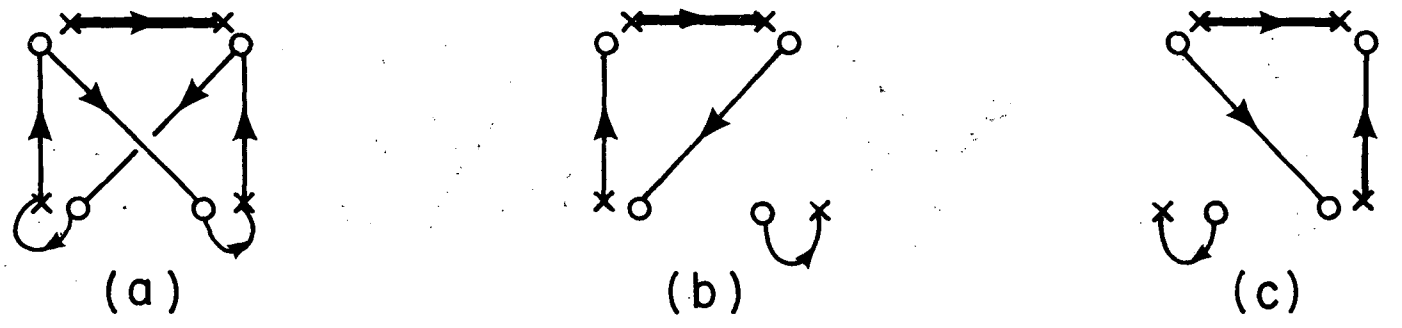

Figure 30

XBL7810-6614

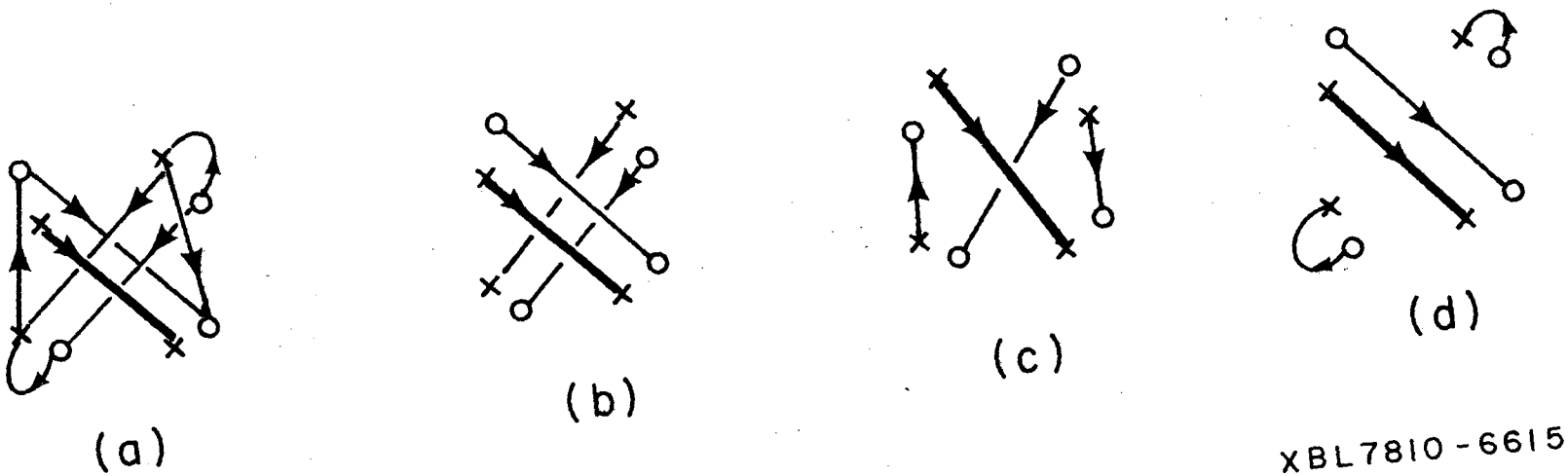

Figure 31

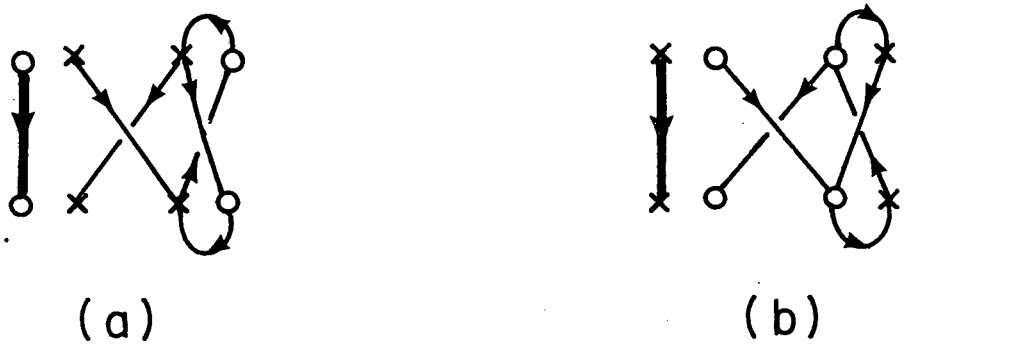

Figure 32

XBL7810-6612

This report was done with support from the Department of Energy. Any conclusions or opinions expressed in this report represent solely those of the author(s) and not necessarily those of The Regents of the University of California, the Lawrence Berkeley Laboratory or the Department of Energy.

TECHNICAL INFORMATION DEPARTMENT
LAWRENCE BERKELEY LABORATORY
UNIVERSITY OF CALIFORNIA
BERKELEY, CALIFORNIA 94720